Bioorganic & Medicinal Chemistry 17 (2009) 4345–4359

Contents lists available at ScienceDirect

Bioorganic & Medicinal Chemistry

journal homepage: www.elsevier.com/locate/bmc

Retinoid receptor subtype-selective modulators through synthetic modifications of RARγ agonists

Susana Álvarez [a], Rosana Álvarez [a], Harshal Khanwalkar [b], Pierre Germain [b], Géraldine Lemaire [b], Fátima Rodríguez-Barrios [a], Hinrich Gronemeyer [b,*], Ángel R. de Lera [a,*]

[a] Departamento de Química Orgánica, Universidade de Vigo, 36310 Vigo, Spain
[b] Department of Cancer Biology—Institut de Génétique et de Biologie Moléculaire et Cellulaire (IGBMC)/CNRS/INSERM/ULP, BP 163, 67404 Illkirch Cedex, C.U. de Strasbourg, France

ARTICLE INFO

Article history:
Received 22 December 2008
Revised 6 May 2009
Accepted 11 May 2009
Available online 18 May 2009

Keywords:
Retinoid receptor subtypes
Antagonists
Arotinoids
Synthesis
Molecular modeling

ABSTRACT

A series of retinoids designed to interfere with the repositioning of H12 have been synthesized to identify novel RARγ antagonists based on the structure of known RARγ agonists. The transcriptional activities of the novel ligands were revealed by cell-based reporting assays, using engineered cells containg RAR subtype-selective fusions of the RAR ligand-binding domains with the yeast GAL4 activator DNA-binding domain and the cognate luciferase reporter gene. Whereas none of the ligands exhibited features of a selective RARγ antagonist, some of them are endowed with interesting activities. In particular **24a** acts as a pan-RAR agonist that induces at high concentration a higher transactivation potential on RARα than TTNPB and synergizes at low concentration with TTNPB-bound RARα but not RARβ or RARγ. Similarly, **24c** synergizes with TTNPB-bound RARγ and exhibits RARα,β antagonist activity. Compounds **24b** and **25b** are strong RARα,β-selective antagonists without agonist or antagonist activities for RARγ. Compounds **24b** and **24c** display weak RXR antagonist activity. In addition several pan-antagonists and partial agonist/antagonists have been defined.

© 2009 Elsevier Ltd. All rights reserved.

1. Introduction

Retinoids, that is, the natural and synthetic derivatives of vitamin A, are powerful signaling molecules that exert their actions on cell growth and differentiation, carcinogenesis, homeostasis and development primarily through binding to the retinoid receptors RARs and RXRs,[1–3] members of the nuclear receptor superfamily.[4,5] Accumulating structural data has provided detailed information on the binding characteristics of agonists, inverse agonists, antagonists and partial agonists, to the point that retinoid receptors are perhaps the best known members of the nuclear receptor (NR) superfamily.[6]

The retinoic acid receptors are important drug targets for cancer therapy and prevention.[7] All-*trans*-retinoic acid (ATRA), the natural ligand for RAR is used as a differentiation agent against acute promyelocytic leukemia. A synthetic RXR agonist LGD1069 (bexarotene, Targretin®) has been approved for the treatment of cutaneous T cell lymphoma[8] and is undergoing clinical trials for other indications.[9] Moreover, the potential of RXR ligands (rexinoids) for the therapy of metabolic diseases through the modulation of the biological effects that are under the control of certain RXR–NR heterodimers is increasingly recognized.[10]

RAR subtypes, expressed from three isotypic genes (α, β and γ), differ in only three residues of the ligand-binding pocket (LBP).[11,12] RARα and RARβ differ by just one residue in helix 3 (S_{232} in RARα; A_{225} in RARβ), whereas RARβ and RARγ diverge in two residues in helices H5 (I_{263} in RARβ; M_{272} in RARγ) and H11 (V_{398} in RARβ; A_{397} in RARγ). H3 and H5 interact with the polyene side-chain, whereas H11 contacts the hydrophobic ring of the retinoid ligand.

Based on numerous structural and functional studies, general guidelines for the design of RAR subtype-selective agonists and antagonists have been established.[12,6,13] RARγ-selective retinoids exhibit the longest connectors between the hydrophobic and the polar ends rings of the arotinoid (or aromatic retinoid) skeleton. The size of the linker directs the hydrophobic ring into the corresponding pocket close to H11 and this causes a decrease in the affinity for RARα/β. Moreover, the RARγ-specific Met_{272} which shows a highly conserved conformation in all solved crystal structures, can engage in hydrogen bonding interactions with suitable functional groups such as those of the RARγ-selective ligands **2**,[14] **3**,[14] **4**,[15] **5**,[16] **6**,[17] and **7**[18] (see Fig. 1).[6,19–21]

The RARγ subtype is highly expressed in the epidermis and has been shown to contribute to primitive endodermal differentiation of F9 murine embryonal carcinoma cells.[22] A partial[23a] and a selective antagonist of RARγ have been reported[23b] but the structure of

* Corresponding authors. Tel.: +33 3 88 65 3473; fax: +33 3 88 65 3437 (H.G.), tel.: +34 986 812316; fax: +34 986 811940 (A.D.L.).
E-mail addresses: hg@igbmc.u-strasbg.fr (H. Gronemeyer), qolera@uvigo.es (Á.R. de Lera).

0968-0896/$ - see front matter © 2009 Elsevier Ltd. All rights reserved.
doi:10.1016/j.bmc.2009.05.035

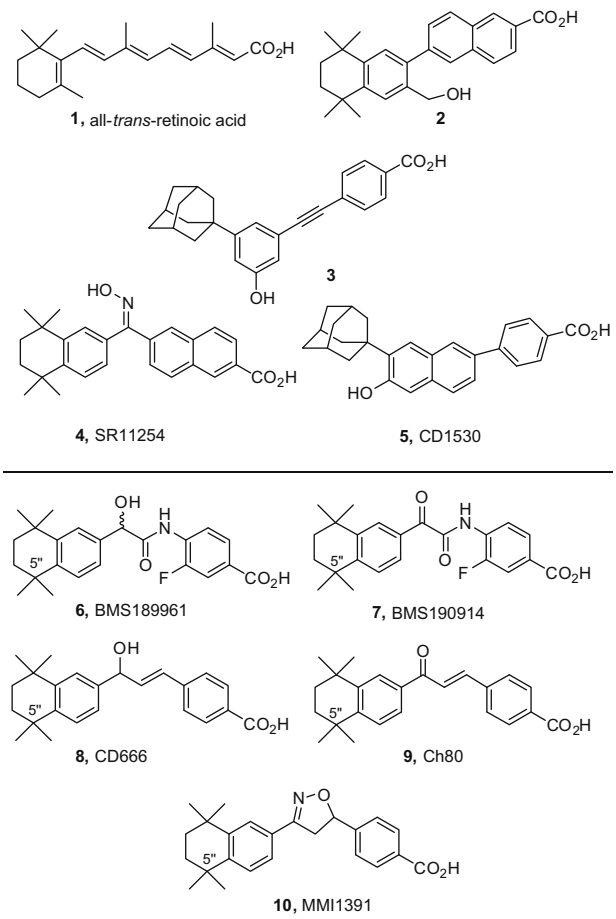

Figure 1. RARγ-selective retinoids (**2**–**5**, **6**, **8**), and RAR-pan agonists (**1**, **7**, **9**, **10**). The last five retinoids have been selected as leads for the design of RARγ-selective antagonists.

the latter was not disclosed. In order to have access to such a pharmacologically relevant tool, we integrated the principles of nuclear receptor antagonism[24] within the structure of some of the best characterized RARγ agonists.[6,12,25] The simplest approach is to place at appropriate positions of the agonist structures substituents that hinder H12 re-positioning. This in turn will impede the release of co-repressors and/or the recruitment of co-activators, two of the key processes linked to transcriptional activation.[24,25]

In the present study we have focused on RARγ-selective agonists with hydroxyalkylamide (BMS189961,[17] **6**) and allyl alcohol (CD666,[16] **8**) functional groups and envisioned synthetic modifications of the hydrophobic region for attaching the 'antagonist' substituents. Through molecular modeling studies (vide infra) position C5″ of the tetramethyltetrahydronaphthalene core suggested itself as optimal for attaching substituents oriented towards H12, an approach pioneered by chemists at Allergan and Bristol–Myers–Squibb.[26,17] Relative to more flexible groups, the rigidity of aryl and alkynyl substituents enforce the directionality. By systematically increasing the length of these groups (phenyl, *p*-tolyl, phenylethynyl), we expected to monitor the transition from agonists to antagonists, in the same manner described for RXR in our previous studies.[27] Along the synthetic sequence analogues of ketoamide **7** and chalcone **9**[28] (the oxidized precursors of **6** and **8**) having the same substitution pattern at C5″ were prepared. Finally, the reactivity of chalcone **9** allows for further diversification, and the C5″-substituted dihydroisoxazole analogues of parent MMI1391 **10**[29] were also prepared.

We report herein the synthesis and characterization of novel retinoids derived from agonists **6**–**10** as well as their characterization using transient transactivation assays. Unexpectedly, no selective RARγ antagonist could be identified within the series of retinoids prepared. However, some of the analogues displayed subtype-selectivities ranging from pan-antagonists to partial agonists/antagonists and 'super-agonists'.

2. Chemistry

The structure of the target arotinoids called for key disconnections involving the generation of the functional groups (chalcone/allyl alcohol/dihydroisoxazole on the one hand, keto/hydroxyalkylamide on the other). The previously described lengthy synthesis of 6-bromodihydronaphthalenone **17** that starts with the Friedel–Crafts acylation of bromobenzene and succinic anhydride **11**[30] was followed (see Supplementary data). Clemensen reduction (Zn, $HgCl_2$, H_2O, HCl, 100 °C) of ketone **12** afforded carboxylic acid **13** (60%), which was converted into the methyl ester **14** (*p*-TsOH, MeOH, benzene, 90 °C, 80%) and the latter transformed into tertiary alcohol **15** using MeMgBr in ether (Scheme 1).

Friedel–Crafts alkylation and tetrahydronaphthalene construction providing **16** (79% yield) took place upon treating **15** with polyphosphoric acid at 50 °C. Finally, a highly efficient (96%) benzylic oxidation of **16** (CrO_3, AcOH, Ac_2O, benzene, 0 °C) afforded 6-bromo-3,4-dihydro-4,4-dimethylnaphthalene-1(2*H*)-one **17**. Addition of Grignard reagents PhMgBr and *p*-tolylMgBr to **17** provided benzyl alcohols **18a** and **b** in 80% and 75% yield, respectively. Likewise, addition of the lithium acetylide derived from ethynylbenzene produced propargylic alcohol **18c** in 77% yield. These alcohols were then efficiently (92–96%) dehydrated to dihydronaphthalenes **19a**–**c** upon refluxing with *p*-TsOH in benzene. Bromine–lithium exchange in **19a**–**c** was followed by trapping the organolithium with DMF to produce aldehydes **20a**–**c** (72% yield), which then were converted into ketones **22a**–**c** in a two-step sequence involving addition of MeLi to **20a**–**c** (77–88%) and oxidation of the benzyl alcohols **21a**–**c** with MnO_2 under basic conditions (87–99%).

Chalcones **24a**–**c** were acquired by the Claisen–Schmidt condensation of ketones **22a**–**c** and ethyl 4-formylbenzoate **23** following the protocol described for the parent system **9** (NaOH, MeOH, 25 °C).[16] The basic reaction conditions produced the saponification of the esters, and therefore the desired carboxylic acids **24a**–**c** were obtained as final products. Allyl alcohols **25a**–**c** were obtained in good yields by treatment of enones **24a**–**c** with Luche's reagent ($NaBH_4$, $CeCl_3{\cdot}7H_2O$, MeOH).[31] Finally, dihydroisoxazole derivatives **26a**–**c** were straightforwardly prepared by reaction of chalcones **24a**–**c** with hydroxylamine ($NH_2OH{\cdot}HCl$, NaOAc, MeOH, 70 °C).

The synthesis of the analogues of selective RARγ agonist BMS189961 **6** is depicted on Scheme 2. The capture of the organolithium resulting from the bromine–lithium exchange reaction of **19a**–**c** with dimethyl oxalate installed the α-ketoester group of **27a**–**c** (52–63%). Due to their instability, ketoesters **27a**–**c** were treated with LiOH to produce **28a**–**c** in moderate to good yields (75–83%).

In situ preparation of the corresponding acid chlorides using doubly-distilled oxalyl chloride was followed by treatment with methyl 4-amino-3-fluorobenzoate **32** (itself obtained from 3-fluoro-4-nitrotoluene **29** via **30** and **31** as described[32]) to afford the ketoamides **33a**–**c** in 51–55% yields. These were reduced with sodium borohydride to the corresponding hydroxyamides **35a**–**c** (80–84%). Lastly, esters **33a**–**c** and **35a**–**c** were converted into the carboxylic acids **34a**–**c** and **36a**–**c** in excellent yields (89–98%) using NaOH in MeOH.

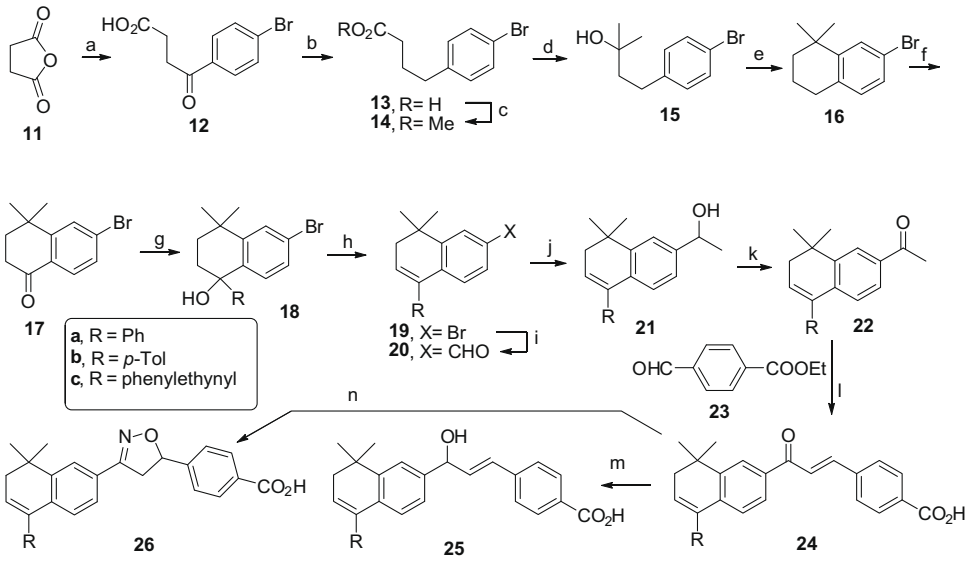

Scheme 1. Reagents and conditions: (a) bromobenzene, $AlCl_3$, 96 h, 93%; (b) Zn–Hg, HCl, H_2O, reflux, 15 h, 60%; (c) *p*-TsOH, C_6H_6, MeOH, reflux, 18 h, 95%; (d) MeMgBr, Et_2O, 24 h, 97%; (e) PPA, 50 °C, 9 h, 71%; (f) CrO_3, Ac_2O, AcOH, 5 h, 70%; (g) PhMgBr, THF, 20 h, 87%; *p*-TolMgBr, THF, 20 h, 80%; *n*-BuLi, ethynylbenzene, THF, 15 h, 77%; (h) *p*-TsOH, C_6H_6, reflux, 2 h (**19a**, 96%; **19b**, 94%; **19c**, 92%); (i) *t*-BuLi, DMF, THF, −78 °C, 5 h (**20a**, 72%; **20b**, 72%; **20c**, 71%); (j) MeLi, THF, 0 °C (**21a**, 77%; **21b**, 88%; **21c**, 83%); (k) MnO_2, Na_2CO_3, CH_2Cl_2 (**22a**, 99%; **22b**, 87%; **22c**, 66%); (l) ethyl 4-formylbenzoate **23**, NaOH, THF (**24a**, 63%; **24b**, 72%; **24c**, 68%); (m) $NaBH_4$, $CeCl_3{\cdot}7H_2O$, MeOH (**25a**, 81%; **25b**, 92%; **25c**, 90%); (n) $NH_2OH{\cdot}HCl$, NaOAc, MeOH, 70 °C (**26a**, 65%; **26b**, 70%; **26c**, 74%).

3. Transcriptional activation studies

To evaluate the effects of the described retinoids on RARα, RARβ, RARγ, and RXRβ- mediated transactivation, a reporter assay with genetically engineered HeLa cell lines[33] that had been stably cotransfected with a chimeric receptor construct and the cognate reporter gene was used. Since the aminoacid residues that constitute the ligand-binding pockets of the RXR subtypes do not differ, the single RXRβ reporter is assumed to reveal the ligand responsiveness as readout for all three RXRs. This reporter assay is based on the generation of a fusion protein, which consists of the ligand-binding domain of the corresponding receptor and the DNA-binding domain of the yeast GAL4 transcription factor. The cells also contain a stably integrated luciferase reporter, which is controlled by five Gal4 response elements in front of a β-globin promoter; this is termed '$(17m)_5$-βG-Luc'.[34,35] The transcriptional activity of the various compounds was compared with the activity of the pan-RAR agonist TTNPB **37** and the RXR-agonist 9-*cis*-retinoic acid **38** (see Fig. 4) as positive controls for RAR (see Supplementary data) and RXR (Fig. 4), respectively. Note that this reporter system is insensitive to endogenous receptors, which cannot recognize the GAL4-binding site.

The analysis reveals a number of interesting features of some of the new retinoids. It is remarkable that **24a** and **24c** act at high concentration as highly potent agonists for RARα and RARγ, respectively, if compared with TTNPB (Fig. 2).[36] This appears not to be due to residual RXR agonist activity (which might have possibly originated from traces of endogenous RXR that is well-established to synergize with retinoids in RAR–RXR heterodimers[4,37]), as **24c** does not display any RXR agonist activity but rather has weak RXR antagonist activity, which is even more pronounced for **24a** (see Supplementary data). While **25b** has no significant RARγ

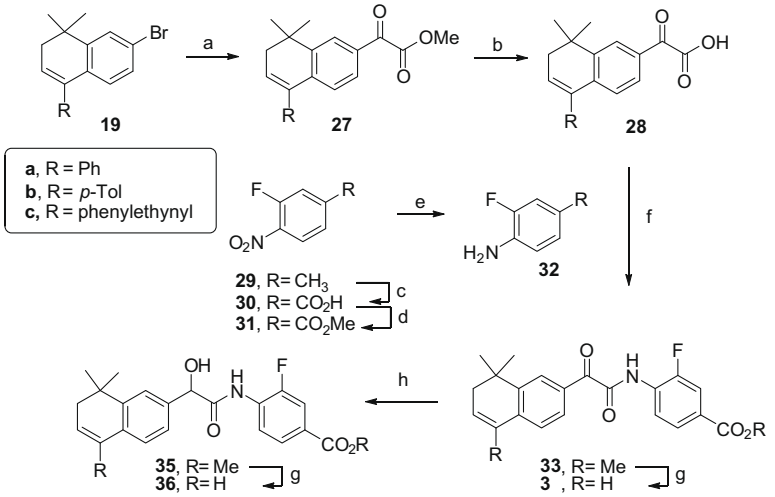

Scheme 2. Reagents and conditions: (a) *t*-BuLi, $(MeOCO)_2$, THF, 10 h (**27a**, 52%; **27b**, 59%; **27c**, 63%); (b) LiOH, THF/H_2O, 80 °C, 2 h (**28a**, 83%; **28b**, 81%; **28c**, 85%); (c) $KMnO_4$, H_2O, 100 °C, 50%; (d) *p*-TsOH, MeOH, reflux, 16 h, 70%; (e) H_2, Pd/C, 45 psi, 45 min, 75%; (f) $(ClCO)_2$, CH_2Cl_2, DMF, Et_3N, AcOEt, 80 °C (**33a**, 52%; **33b**, 51%; **33c**, 55%); (g) 10 N NaOH, MeOH, 23 °C (**34a**, 90%; **34b**, 91%; **34c**, 89%; **36a**, 98%; **36b**, 90%; **36c**, 91%); (h) $NaBH_4$, MeOH, AcOEt (**35a**, 84%; **35b**, 80%; **35c**, 80%).

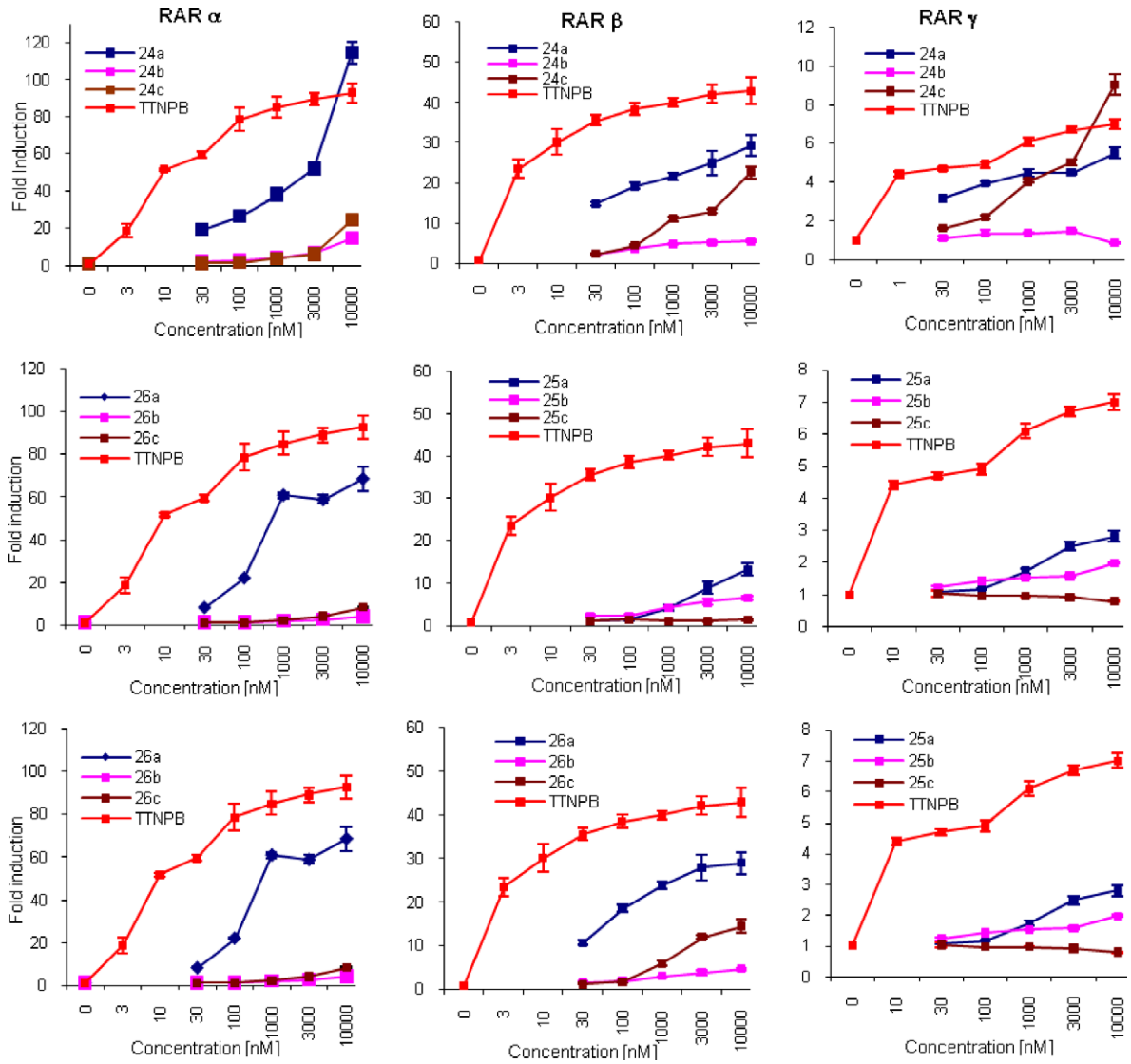

Figure 2. Dose–response luciferase reporter cell assays (fold-induction) revealing the RAR subtype agonist activities of the retinoids **24**–**26**. For details on the assay system, see Section 5. The data are derived from at least three independent experiments; the standard deviations are indicated.

activity, it is a strong RARα antagonist (RARα, IC_{50} = 400nM, that is, 50% inhibition of 10nM TTNPB-induced activity at 400nM) and displays also significant RARβ antagonist activity (RARβ, IC_{50} = 2 μM) (Figs. 2 and 3). Virtually the same is true for **24b** (RARα, IC_{50} < 300nM; RARβ, IC_{50} = 400nM). It is interesting to note from the perspective of RARγ, that **26c** is a moderate (IC_{50} = 3 μM) and **26a** a weak (IC_{50} > 10 μM) antagonist, while **26b** is inactive.

The **34a,b,c** series corresponds to pan-RAR antagonists (see Supplementary data) which however display high RXR agonist activity (see Supplementary data); in contrast **36a** is a partial agonist with lower activity than TTNPB (see Supplementary data) and (similarly to **36c**) a weak pan-RAR antagonist with no RXR agonist activity detected. **36b** is neither agonist nor antagonist and may not significantly bind to RARs or RXR. In contrast to **36a** analog **36c** does not possess any significant RAR agonist activity (see Supplementary data).

4. Discussion

A great number of structural and functional studies have provided a series of guidelines for the design of RAR subtype-selective agonists and antagonists.[12,6,13] For example, RARα agonists are characterized by the presence of amide bonds in the linker between a hydrophobic ring and a benzoic acid terminus, which are considered to participate in hydrogen bonding interactions with the subtype-determining Ser232. In addition, small halogen atoms (F) at the *ortho* position of the benzoic acid improve RARα selectivity. RARβ selectivity[38] is expected for retinoids with bulkier hydrophobic rings capable of filling the enlarged ligand-binding pocket between H5 and H10 that results from the orientation of Ile263 away from the ligand, as observed in the crystal structure, and is further increased by halogen atoms (Cl) at the *meta* position of the benzoic acid.[13] On the other hand, RARγ selectivity is exhibited by retinoids with longer (one additional atom) connectors between the hydrophobic and the polar ends of the skeleton in particular if these functional groups have hydrogen bond donors. The gain in RARγ selectivity is considered to result from the hydrogen bonding interactions with the subtype-specific Met272 residue, a structural feature that is highly conserved in all crystal structures determined.[6,19–21]

Although an RARγ-selective antagonist has been described,[23b] the structure of this compound has not been disclosed. Moreover,

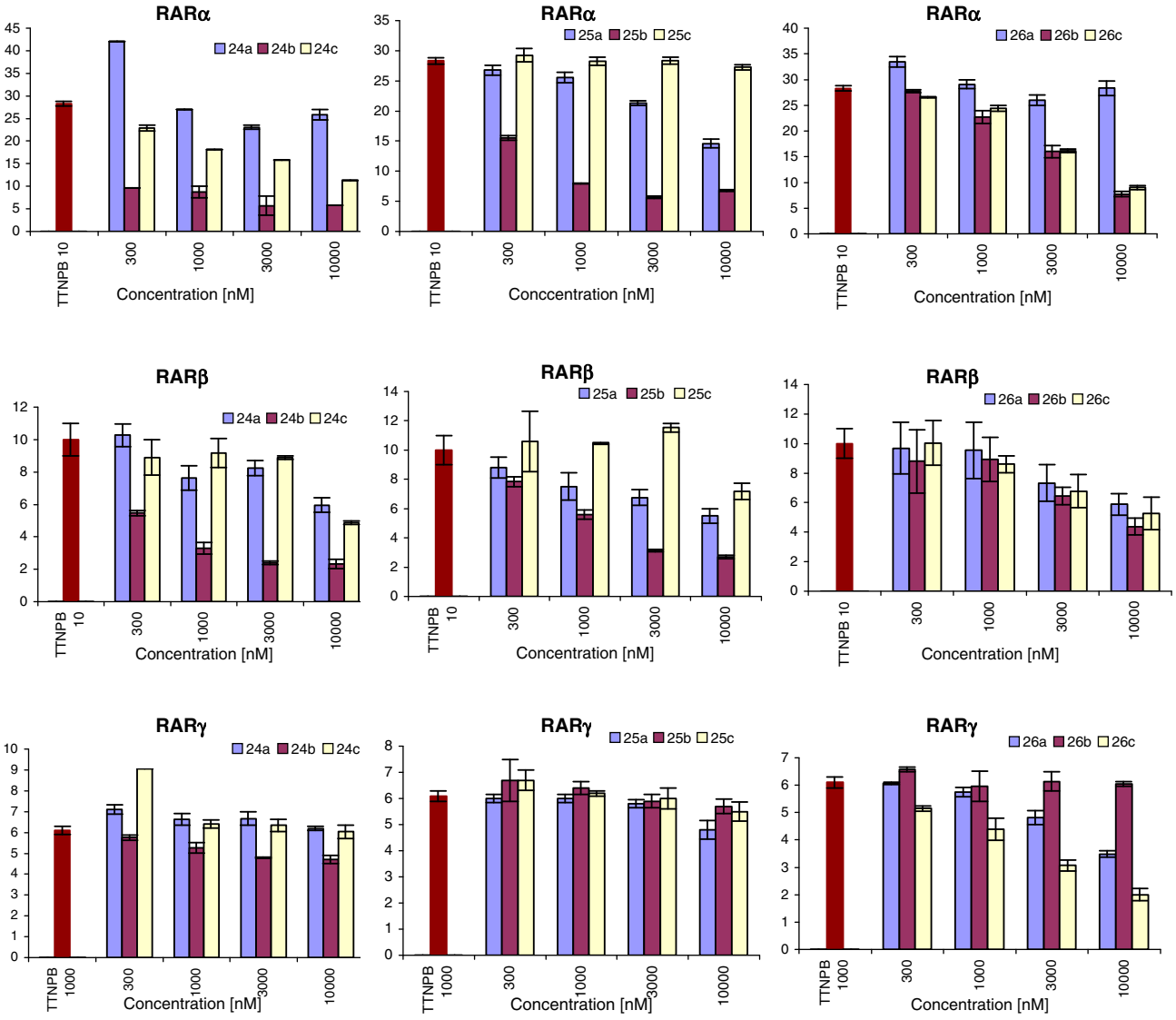

Figure 3. Dose–response luciferase reporter cell assays revealing the RAR subtype antagonist activities of the retinoids **24**–**26**. The agonist TTNPB (10 nM) (compound **37**, Fig. 4) was challenged with increasing amounts of the various retinoids and luciferase activity was determined. The decreased activity relative to TTNPB reveals antagonism. For further details on the assay system, see Section 5. The data are derived from at least three independent experiments; the standard deviations are indicated.

no structure of an antagonist-bound complex with resolution at the atomic level is currently available. Only the selective antagonist BMS195614 (**39**, Fig. 4) bound to RARα when forming a heterodimer with the constitutively active mutant mRXRαF318A bound to oleic acid (PDB code: 1dkf) has yielded a crystal structure.[39] To aid the synthetic design this complex was used as a starting structure for modeling the ligand-binding domain of the human RARγ-antagonist-bound conformation. The protocol is described in detail in Section 5. Docking known RARγ-selective agonists (BMS189961 **6**, CD666 **8**; see Fig. 1), in this model suggested that the 'antagonist' substituent should be placed at the C5″ position of the tetrahydronaphthalene ring. Based on this assumption, a collection of fifteen retinoids having in common an 'antagonist' substituent at C5″ of increasing size and defined orientation (phenyl, *p*-tolyl and 4-phenylethynyl) but differing in the nature of the connector and polar groups were synthesized.

Transient transactivation studies of these ligands afforded activity profiles which are difficult to reconcile with the modeling and design principles. First of all, none of the retinoids could be classified as RARγ-selective antagonist. The greatest discrimination

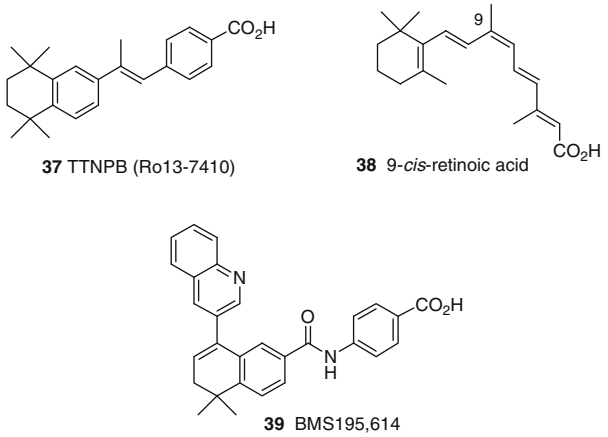

37 TTNPB (Ro13-7410)

38 9-*cis*-retinoic acid

39 BMS195,614

Figure 4. Structures of the RAR agonist (**37**) and RXR agonist (**38**) used as standards in the transactivation assays, and the RARα-selective antagonist (**39**).

of RARγ vs its paralogues was found for the dihydroisoxazole series **26**. Whereas **26a** is a RARγ antagonist of moderate potency, **26c** is a stronger antagonist, whereas **26b** is inactive. This selectivity is consistent with molecular modeling studies in which analogue **26a** was docked into the antagonist-bound RARγ structure constructed by homology and then minimized. Since the ligand was synthesized as a racemate, both enantiomers of **26a** were docked into the RARγ binding pocket. Only the *S* enantiomer afforded reasonable energy values upon minimization, and molecular dynamics studies were carried on with this enantiomer. The agonist core of (*S*)-**26a** is buried in a predominantly hydrophobic pocket corresponding essentially to the all-*trans*-retinoic acid binding niche in the holo-RARγ LBD structure.[40,41] Residues located in H1, H3, H5, the β turn, loop L6–7, and H11 form the agonist cavity. The C5″-phenyl moiety of (*S*)-**26a**, which is almost perpendicular to the dihydronaphthalene part of the ligand, protrudes from the agonist pocket between H12 (Leu411, Ile412), H11 (Ala394, Ala397), L11–12 (Met408), and H3 (Trp227, Ser231, Ala234, Thr235, Ile238). All these residues make van der Waals contacts with the ligand, particularly with the phenyl group at C5″. The resulting model of RARγ in complex with (*S*)-**26a** was refined using energy minimization and its dynamic behavior was simulated using unrestrained Molecular Dynamics to assess the feasibility of the proposed complexes. As seen in Figure 5, the bulky phenyl group at the C5″ position is directed towards the H11–H12 region, thus stabilizing the antagonist conformation of the receptor. Moreover, a comparison between the reported crystal structure of RARα-BMS195614 (**39**) and the model of RARγ-(*S*)-**26a** justifies the experimentally determined moderate subtype selectivity of the latter as a racemate. The small Ala397 group in RARγ is replaced by the bulkier Val395 in RARα and Val388 in RARβ, which interact with the added substituent at C5″ (see Fig. 5). Nevertheless the antagonist does not maintain the hydrogen bonding to the subtype-discriminating Met_{272} due to the different occupancy of the binding pocket, and thus the RARγ-subtype selectivity is eroded.

On the other hand, the ketoamides derived from 3-fluorobenzoic acid (**34a**–**c**) proved to be pan-RAR-antagonists, a profile shared by the corresponding hydroxyalkylamides although at higher concentrations. It is puzzling that the parent retinoid BMS189961 (**6**, as a racemate) is a potent and selective RARγ agonist, an activity due to the (*R*)-enantiomer BMS270394,[41] whereas its derivatives **36** are unselective antagonists.

The series of compounds **25** formally derive from the structure of allyl alcohol CD666 (**8**), another known RARγ agonist.[42,20] Compound **25b**, with a *p*-tolyl group at C5″ behaves as a dual RARα and RARβ antagonist, with greater potency for the former, while devoid of RARγ agonistic activity. The same properties are exhibited by the corresponding chalcone **24b** with the same C5″-substituent, formally derived from pan-agonist Ch80 (**9**). Interestingly, the analogues of **24b** with phenyl (**24a**) and phenylethynyl (**24c**) groups displayed the remarkable property of inducing higher maximum transactivation at high concentration than the powerful pan-agonist TTNPB (**37**) in RARα and RARγ, respectively. This could be explained by a scenario in which **24a** has a lower affinity to RARα than TTNPB but is more efficient at inducing a conformation that allows coactivator recruitment and/or facilitates corepressor release. A similar rationale for **24c** would explain its strong agonist activity for RARγ at high concentrations. It is remarkable that these two ligands at low concentration enhance the transactivation induced by TTNPB for those receptors where they exhibit the enhanced agonist activity at high concentration. While we have no immediate explanation for this phenomenon, we speculate that at low concentration (300 nM in Fig. 3) they may be a coexistence of TTNPB and **24a**-bound RARα. The **24a**-bound receptors may efficiently recruit coactivator complexes but display a rapid release from the target promoter due to high dissociation rate of the ligand. In this case long-lived TTNPB-bound RARα, which is less efficient at coactivator recruitment, may take over the pre-established complexes from the **24a**-bound RARα, resulting in apparent ligand synergy on a single receptor species. Towards higher concentrations of the strong agonist increasingly less TTNPB-bound receptors are available such that only **24a**-bound receptors drive the recruitment process. Retinoid **24c** shows the same property with TTNPB-bound RARγ, and moreover has RARα,β-antagonist activity. This selectivity profile is unprecedented in retinoid receptor ligands.

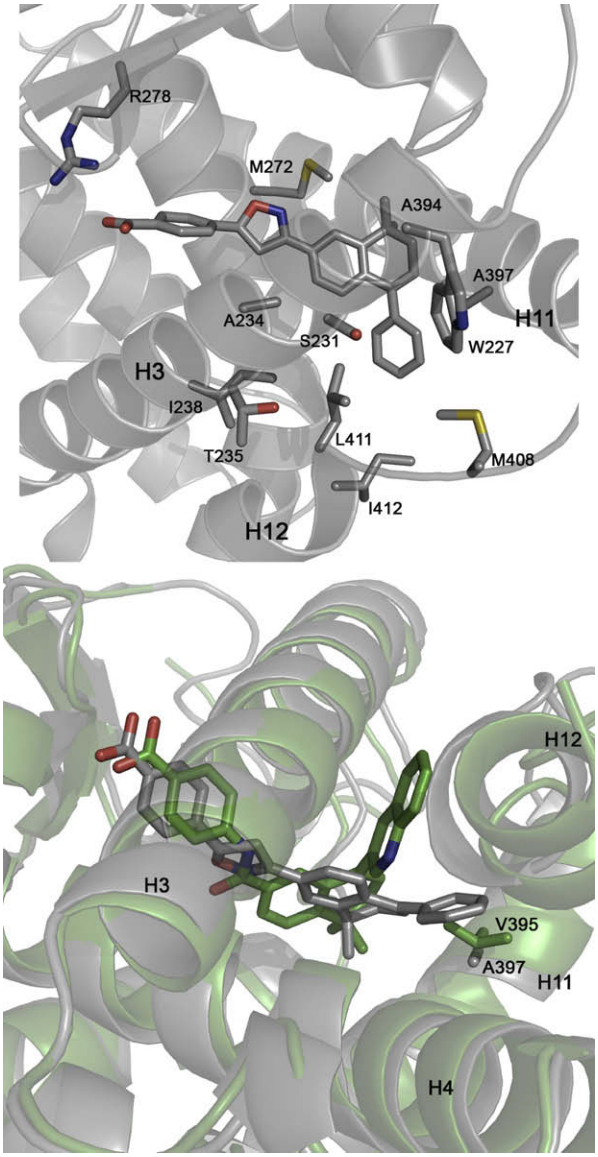

Figure 5. Top: Minimized structure obtained after docking (*S*)-**26a** in the RARγ-binding pocket; the side chains of the aminoacids that make contact with the ligand are highlighted. Bottom: Close-up view of the superimposed minimized structures of the complexes (*S*)-**26a**-RARγ (gray) and BMS614 (**9**)-RARα (green). The subtype-specific Ala397 (RARγ) and Val395 (RARα) residues at H11 are labeled.

We do not believe that the effects of chalcones **24** are due to the synergistic activation of RXR.[36] RXR ligands or rexinoids on their own activate 'permissive' heterodimers (e.g., PPAR/RXR) but, due to a phenomenon referred to as 'RXR subordination' generally not 'non-permissive' heterodimers (e.g. RXR/RAR).[35] Selective RXR modulators, that is, rexinoid ligands that activate a particular subset of heterodimers, have been described for PPAR and RAR heterodimers.[36,6] Certain rexinoids act as synergists[36] for transactiva-

tion through RAR and enhance the cell differentiation induced by synthetic retinoids.[43–46] However, the synergistic activities of **24a** and **24c** seem to be unrelated to RXR transactivation, since they behave rather as antagonists of RXR. More subtle and possibly kinetic phenomena are likely operating in this case as suggested above. The effect of ligands on the mechanism of transactivation must in fact be analyzed in the context of the relative stability of the ligand–nuclear receptor complexes with their co-regulators (co-repressors or co-activators). This complex is an ensemble of proteins and enzymes that includes histone deacetylases and histone acetyl transferases that in turn induces chromatin remodeling and transcriptional activation.[47]

To conclude, strong agonists selective for the RARα and RARγ subtypes have been discovered from transactivation studies of a collection of retinoids designed to acquire antagonistic properties starting from the structure of RARγ-selective agonists. Whereas in general the synthetic retinoids displayed antagonistic profiles with moderate or no selectivity, a series (**24a**–**c**) are endowed with the ability to activate transcription through a specific RARα or RARγ subtype at higher values than pan-agonist TTNPB (**37**). It is interesting to note that the crystal structure of parent pan-agonist chalcone Ch80 (**9**, Fig. 1)[20] bound to RARγ reveals a *s-trans* conformation about the bond joining the carbonyl group to the double bond.[20] The increase in the number of rotatable bonds in the central connector region of the retinoids **24**, **25**, **34** and **36** increases the conformational freedom of the ligand relative to more rigid analogues (such as, for example, compounds **2**–**5**). The increase in flexibility makes the computational-based prediction of the ligand activity less accurate, as shown in this work with the RARγ-inspired antagonists **24**–**26**, **34** and **36**. Computational chemists are increasingly paying attention to the importance of the target flexibility in the description of receptor-ligand interactions.[48] At present we are still facing the difficulty that the current structural tools (X-ray crystallography, NMR spectroscopy and molecular dynamics) still provide too limited information to accurately describe ligand–receptor complexes and their biological readouts which adds uncertainty to the prediction of the properties (agonists, antagonist) of ligands as exemplified by the present report.

5. Experimental

5.1. General

Solvents were dried according to published methods and distilled before use. HPLC grade solvents were used for the HPLC purification. All other reagents were commercial compounds of the highest purity available. All reactions were carried out under argon atmosphere, and those not involving aqueous reagents were carried out in oven-dried glassware. Analytical thin layer chromatography (TLC) was performed on aluminium plates with Merck Kieselgel 60F_{254} and visualized by UV irradiation (254 nm) or by staining with an ethanolic solution of phosphomolibdic acid. Flash column chromatography was carried out using Merck Kieselgel 60 (230–400 mesh) under pressure. Infrared spectra were obtained on a spectrophotometer, from a thin film deposited onto a NaCl glass. ^{1}H NMR spectra were recorded in $CDCl_3$, CD_2Cl_2, and CD_3OD at ambient temperature on a spectrometer at 400 MHz with residual protic solvent as the internal reference [$CDCl_3$, δ_H = 7.26 ppm; CD_2Cl_2, δ_H = 5.30 ppm; CD_3OD, δ_H = 3.31 ppm); chemical shifts (δ) are given in parts per million (ppm), and coupling constants (J) are given in hertz (Hz). The proton spectra are reported as follows: δ (multiplicity, coupling constant J, number of protons, assignment). ^{13}C NMR spectra were recorded in $CDCl_3$ and CD_2Cl_2 or CD_3OD at ambient temperature at 100 MHz, with the central peak of $CDCl_3$ (δ_C = 77.0 ppm), CD_2Cl_2 (δ_C = 54.2 ppm) or CD_3OD (δ_C = 49.05 ppm) as the internal reference. DEPT135 pulse sequences were used to aid in the assignment of signals in the ^{13}C NMR spectra. Mass Spectra were obtained on a instrument operating at 70 eV by electron ionization. FAB experiments were performed on a instrument using 3-nitrobenzylalcohol or glycerol as matrices.

5.2. 6-Bromo-4,4-dimethyl-1,2,3,4-tetrahydro-1-phenyl-(1*H*)-naphthalen-1-ol (18a)

To a solution of 6-bromo-4,4-dimethyl-1,2,3,4-tetrahydro-(1*H*)-naphthalen-1-one **17**[30] (1.5 g, 5.9 mmol) in THF (19 mL) was added phenylmagnesium bromide (9.0 mL, 1 M in THF, 9.0 mmol) and the mixture was stirred for 22 h at 25 °C. A 5% aqueous HCl solution was added and the mixture was extracted with *t*-BuOMe (3×). The combined organic layers were washed with H_2O (3×) and brine (3×) and dried ($Na_2S_2O_3$) and the solvent was removed. The residue was purified by chromatography (silica gel, 95:5 hexane/AcOEt) to afford 1.71 g (87%) of a white solid identified as **18a**. Mp: 105 °C (Et_2O/hexane). Elemental Anal. Calcd for $C_{18}H_{19}BrO$: C, 65.27; H, 5.78. Found: C, 65.09; H, 5.79. ^{1}H NMR (400.16 MHz, $CDCl_3$): δ 7.54 (d, J = 2.0 Hz, 1H), 7.4–7.2 (m, 6H), 6.97 (d, J = 8.4 Hz, 1H), 2.23 (ddd, J = 13.5, 10.1, 3.1 Hz, 1H), 2.12 (ddd, J = 12.3, 8.2, 3.0 Hz, 1H), 1.88 (ddd, J = 13.3, 10.0, 2.9 Hz, 1H), 1.58 (ddd, J = 11.3, 8.2, 3.1 Hz, 1H), 1.40 (s, 3H), 1.28 (s, 3H) ppm. ^{13}C NMR (100.62 MHz, $CDCl_3$): δ 148.6 (s), 148.2 (s), 139.8 (s), 130.6 (d), 129.5 (d), 129.2 (d), 127.8 (d, 2×), 126.8 (d), 126.3 (d, 2×), 121.9 (s), 75.4 (s), 37.3 (t), 34.5 (t), 34.2 (s), 31.3 (q), 31.2 (q) ppm. MS (EI$^+$): *m/z* (%) 332 (M$^+$, 16), 330 (M$^+$, 16), 255 (13), 253 (25), 252 (100), 251 (13), 219 (10), 218 (45), 115 (12), 105 (10), 91 (11), 77 (23). HRMS (EI$^+$): calcd for $C_{18}H_{19}{}^{79}BrO$, 330.0619; found, 330.0633. IR (NaCl): ν 3416 (w, OH), 2959 (w, C–H) cm^{-1}. UV (MeOH): λ_{max} 230 nm.

5.3. 6-Bromo-4,4-dimethyl-1,2,3,4-tetrahydro-1-*p*-tolyl-(1*H*)-naphthalen-1-ol (18b)

Following the above procedure, the reaction of **17** (1.5 g, 5.9 mmol) and *p*-tolylmagnesium bromide (9 mL, 1 M in THF, 8.8 mmol) in THF (19 mL) afforded, after purification by chromatography (silica gel, 95:5 hexane/AcOEt), 1.63 g (80%) of a white solid identified as **18b**. Mp: 101 °C (Et_2O/hexane). Elemental Anal. Calcd for $C_{19}H_{21}BrO$: C, 66.09; H, 6.13. Found: C, 66.20; H, 6.15. ^{1}H NMR (400.16 MHz, $CDCl_3$): δ 7.29 (dd, J = 8.5, 2.0 Hz, 1H), 7.19 (s, 1H), 7.17 (d, J = 8.3 Hz, 1H), 7.2–7.0 (m, 4H), 2.54 (s, 3H), 2.11 (ddd, J = 13.5, 9.1, 3.2 Hz, 1H), 2.09 (ddd, J = 12.1, 9.0, 3.1 Hz, 1H), 1.72 (ddd, J = 13.8, 9.2, 3.1 Hz, 1H), 1.47 (ddd, J = 12.3, 9.0, 3.2 Hz, 1H), 1.25 (s, 3H), 1.22 (s, 3H) ppm. ^{13}C NMR (100.62 MHz, $CDCl_3$): δ 145.6 (s), 145.5 (s), 143.8 (s), 137.0 (s), 131.7 (d), 131.4 (d), 128.8 (d, 2×), 128.7 (d), 126.8 (d, 2×), 120.2 (s), 76.0 (s), 37.9 (t), 35.1 (t), 34.3 (s), 31.8 (q), 31.7 (q), 21.4 (q). MS (EI$^+$): *m/z* (%) 346 (M$^+$, 2), 344 (M$^+$, 2), 328 (52), 326 (58), 313 (26), 311 (31), 283 (48), 255 (42), 253 (48), 232 (100), 217 (53), 215 (51), 202 (50), 115 (18), 81 (46), 69 (53). HRMS (EI$^+$): calcd for $C_{19}H_{21}{}^{79}BrO$, 344.0776; found, 344.0785. IR (NaCl): ν 3432 (w, OH), 3058–2863 (s) cm^{-1}. UV (MeOH): λ_{max} 232 nm.

5.4. 6-Bromo-4,4-dimethyl-1,2,3,4-tetrahydro-1-(2-phenylethynyl)-(1*H*)-naphthalen-1-ol (18c)

To a cooled (0 °C) solution of 1-ethynylbenzene (0.96 g, 9.5 mmol) in THF (60 mL) was added *n*-BuLi (6.5 mL, 1.45 M in hexane, 9.46 mmol). After 30 min, a solution of **17** (2.0 g, 7.88 mmol) in THF (40 mL) was added and the mixture was stirred for 20 h at 25 °C. After cooling down to 0 °C, H_2O was added and the mixture was extracted with *t*-BuOMe (3×). The combined organic layers were dried (Na_2SO_4) and the solvent was removed.

The residue was purified by chromatography (silica gel, 95:5 hexane/AcOEt) to afford 2.16 g (77%) of a white solid identified as **18c**. Mp: 106 °C (Et_2O/hexane). Elemental Anal. Calcd for $C_{20}H_{19}BrO$: C, 67.61; H, 5.39. Found: C, 67.91; H, 5.69. ^1H NMR (400.16 MHz, CDCl3): δ 7.73 (dd, J = 8.5, 1.0 Hz, 1H), 7.5–7.3 (m, 7H), 2.36 (ddd, J = 10.5, 9.9, 2.9 Hz, 1H), 2.3–2.2 (m, 1H), 1.99 (ddd, J = 11.0, 9.3, 3.0 Hz, 1H), 1.87 (ddd, J = 7.0, 5.4, 3.1 Hz, 1H), 1.36 (s, 3H), 1.33 (s, 3H) ppm. ^{13}C NMR (100.62 MHz, $CDCl_3$): δ 146.9 (s), 137.1 (s), 131.5 (d, 2×), 129.6 (d), 129.5 (d), 129.5 (d), 128.4 (d, 2×), 128.1 (d), 122.5 (s), 122.3 (s), 92.8 (s), 84.6 (s), 35.2 (t), 34.2 (t), 34.1 (s), 31.2 (q), 31.1 (q) ppm. MS (EI^+): m/z (%) 356 (M^+, 5), 354 (M^+, 5), 338 (32), 336 (30), 323 (34), 321 (32), 243 (25), 242 (100), 241 (43), 240 (16), 239 (37), 228 (15), 226 (24), 215 (26), 115 (20). HRMS (EI^+): calcd for $C_{20}H_{19}{}^{79}BrO$, 354.0619; found, 354.0622. IR (NaCl): ν 3396 (w, OH), 3083 (s, C–H) cm^{-1}. UV (MeOH): λ_{max} 235 nm.

5.5. 6-Bromo-3,4-dihydro-4,4-dimethyl-1-phenylnaphthalene (19a)

5.5.1. General procedure for the acid-catalyzed dehydration

To a solution of **18a** (1.71 g, 5.16 mmol) in C_6H_6 (41 mL) placed in a flask equiped with a Dean–Stark apparatus was added *p*-toluenesulfonic acid (0.01 g, 0.052 mmol). After 2 h refluxing, H_2O was added and the mixture was extracted with Et_2O (3×). The combined organic layers were dried (Na_2SO_4) and the solvent was removed. The residue was purified by chromatography (silica gel, hexane) to afford 1.24 g (96%) of a white solid identified as **19a**. Mp: 71 °C (Et_2O/hexane). ^1H NMR (400.16 MHz, $CDCl_3$): δ 7.73 (d, J = 1.7 Hz, 1H), 7.7–7.6 (m, 5H), 7.47 (dd, J = 8.3, 1.9 Hz, 1H), 7.14 (d, J = 8.3 Hz, 1H), 6.25 (t, J = 4.6 Hz, 1H), 2.60 (d, J = 4.6 Hz, 2H), 1.81 (s, 6H) ppm. ^{13}C NMR (100.62 MHz, $CDCl_3$): δ 147.3 (s), 140.4 (s), 138.6 (s), 132.7 (s), 128.6 (d, 2×), 128.5 (d), 128.2 (d, 2×), 127.6 (d), 127.1 (d), 126.9 (d), 126.6 (d), 121.2 (s), 38.6 (t), 33.7 (s), 27.9 (q, 2×) ppm. MS (EI^+): m/z (%) 314 (M^+, 57), 312 (M^+, 57), 299 (20), 297 (20), 270 (20), 268 (19), 233 (13), 219 (19), 218 (100), 217 (16), 215 (15), 203 (20), 202 (25). HRMS (EI^+): calcd for $C_{18}H_{17}{}^{79}Br$, 312.0514; found, 312.0514. IR (NaCl): ν 2925 (m, C–H) cm^{-1}. UV (MeOH): λ_{max} 263 nm.

5.6. 6-Bromo-3,4-dihydro-4,4-dimethyl-1-*p*-tolylnaphthalene (19b)

Following the general procedure, the reaction of **18b** (1.25 g, 3.62 mmol) and *p*-toluenesulfonic acid (0.008 g, 0.040 mmol) in C_6H_6 (29 mL) afforded, after purification by chromatography (silica gel, hexane), 1.12 g (94%) of a white solid identified as **19b**. Mp: 80 °C (Et_2O/hexane). Elemental Anal. Calcd. for $C_{19}H_{19}Br$: C, 69.73; H, 5.95. Found: C, 69.57; H, 5.92. ^1H NMR (400.16 MHz, $CDCl_3$): δ 7.37 (s, 1H), 7.2–7.1 (m, 5H), 6.81 (d, J = 8.6 Hz, 1H), 5.87 (t, J = 4.6 Hz, 1H), 2.30 (s, 3H), 2.23 (d, J = 4.6 Hz, 2H), 1.23 (s, 6H) ppm. ^{13}C NMR (100.62 MHz, $CDCl_3$): δ 147.3 (s), 138.5 (s), 137.4 (s), 136.8 (s), 132.8 (s), 128.9 (d, 2×), 128.6 (d), 128.4 (d, 2×), 127.7 (d), 126.9 (d), 126.1 (d), 121.2 (s), 38.6 (t), 33.7 (s), 27.9 (q, 2×), 21.0 (q) ppm. MS (EI^+): m/z (%) 328 (M^+, 54), 326 (M^+, 57), 313 (20), 311 (20), 284 (32), 283 (32), 247 (12), 233 (23), 232 (100), 217 (22), 215 (24), 202 (21). HRMS (EI^+): calcd for $C_{19}H_{19}{}^{79}Br$, 326.0670; found, 326.0670. IR (NaCl): ν 2927 (m, C–H) cm^{-1}. UV (MeOH): λ_{max} 273 nm.

5.7. 6-Bromo-3,4-dihydro-4,4-dimethyl-1-(2-phenylethynyl)-naphthalene (19c)

Following the general procedure, the reaction of **18c** (1.78 g, 5.15 mmol) and *p*-toluenesulfonic acid (0.01 g, 0.051 mmol) in C_6H_6 (41 mL) afforded, after purification by chromatography (silica gel, hexane), 1.54 g (92%) of a white solid identified as **19c**. M.p.: 68 °C (Et_2O/hexane). Elemental Anal. Calcd. for $C_{20}H_{17}Br$: C, 71.23; H, 5.08. Found: C, 71.80; H, 5.00. ^1H NMR (400.16 MHz, $CDCl_3$): δ 7.52 (d, J = 8.2 Hz, 1H), 7.78 (d, J = 7.7 Hz, 1H), 7.4–7.2 (m, 5H), 7.21 (s, 1H), 6.44 (t, J = 4.8 Hz, 1H), 2.29 (d, J = 4.8 Hz, 2H), 1.20 (s, 6H) ppm. ^{13}C NMR (100.62 MHz, $CDCl_3$): δ 142.6 (s), 135.5 (d), 133.5 (s), 131.6 (d, 2×), 130.9 (d), 128.5 (d, 2×), 128.4 (d), 128.3 (d), 125.6 (d), 123.2 (s), 120.5 (s), 120.2 (s), 90.8 (s), 86.6 (s), 38.9 (t), 33.3 (s), 28.4 (q, 2×) ppm. MS (EI^+): m/z (%) 338 (M^+, 59), 336 (M^+, 61), 323 (44), 322 (12), 321 (44), 295 (16), 292 (18), 257 (15), 243 (24), 242 (100), 241 (35), 229 (27), 68 (14). HRMS (EI^+): calcd for $C_{20}H_{17}{}^{79}Br$, 336.0514; found, 336.0515. IR (NaCl): ν 2961 (m, C–H) cm^{-1}. UV (MeOH): λ_{max} 258, 267 nm.

5.8. 7,8-Dihydro-8,8-dimethyl-5-phenylnaphthalene-2-carbaldehyde (20a)

5.8.1. General procedure for formylation of organolithium intermediates derived from arylbromides

To a cooled (−78 °C) solution of **19a** (0.4 g, 1.53 mmol) in THF (22 mL) was added *t*-BuLi (1.8 mL, 1.7 M in pentane, 3.06 mmol). After 30 min, DMF (0.35 mL, 4.59 mmol) was added and the mixture was stirred for a further 5 h at −78 °C. After cooling down to ambient temperature, a saturated aqueous solution of NH_4Cl was added and the mixture was extracted with Et_2O (3×). The combined organic layers were dried (Na_2SO_4) and the solvent was removed. The residue was purified by chromatography (silicagel, 95:5 hexane/AcOEt) to afford 0.29 g (72%) of a yellow solid identified as **20a**. Mp: 77 °C (Et_2O/hexane). ^1H NMR (400.16 MHz, $CDCl_3$): δ 9.99 (s, 1H), 7.90 (s, 1H), 7.61 (d, J = 7.9 Hz, 1H), 7.4–7.3 (m, 5H), 7.19 (d, J = 7.9 Hz, 1H), 6.18 (t, J = 4.6 Hz, 1H), 2.44 (d, J = 4.6 Hz, 2H), 1.42 (s, 6H) ppm. ^{13}C NMR (100.62 MHz, $CDCl_3$): δ 191.9 (d), 145.8 (s), 140.0 (s), 139.7 (s), 139.0 (s), 135.3 (s), 130.0 (d), 128.5 (d, 2×), 128.3 (d), 128.3 (d, 2×), 127.3 (d), 126.4 (d), 124.5 (d), 38.7 (t), 33.6 (s), 27.9 (q, 2×) ppm. MS (EI^+): m/z (%) 262 (M^+, 36), 247 (19), 234 (49), 233 (34), 220 (20), 219 (100), 218 (32), 217 (11), 215 (11), 205 (13), 204 (41), 203 (28), 202 (28), 192 (10). HRMS (EI^+): calcd for $C_{19}H_{18}O$, 262.1358; found, 262.1352. IR (NaCl): ν 3055 (w, C–H) cm^{-1}. UV (MeOH): λ_{max} 234, 278 nm.

5.9. 7,8-Dihydro-8,8-dimethyl-5-*p*-tolyl-naphthalene-2-carbaldehyde (20b)

Following the general procedure, the reaction of **19b** (0.3 g, 0.92 mmol), *t*-BuLi (1.1 mL, 1.7 M in pentane, 1.84 mmol) and DMF (0.21 mL, 2.76 mmol) in THF (13 mL) afforded, after purification by chromatography (silica gel, 95:5 hexane/AcOEt), 0.18 g (72%) of a white solid identified as **20b**. Mp: 83 °C (Et_2O/hexane). Elemental Anal. Calcd for $C_{20}H_{19}O$: C, 86.92; H, 7.29. Found: C, 86.90; H, 7.29. ^1H NMR (400.16 MHz, $CDCl_3$): δ 10.21 (s, 1H), 8.11 (d, J = 1.3 Hz, 1H), 7.83 (dd, J = 8.2, 1.6 Hz, 1H), 7.5–7.4 (m, 4H), 7.43 (d, J = 8.0 Hz, 1H), 6.38 (t, J = 4.6 Hz, 1H), 2.65 (s, 3H), 2.44 (d, 2H), 1.63 (s, 6H) ppm. ^{13}C NMR (100.62 MHz, $CDCl_3$): δ 191.9 (d), 145.9 (s), 139.8 (s), 138.9 (s), 137.1 (s), 137.0 (s), 135.2 (s), 129.6 (d), 128.9 (d, 2×), 128.4 (d, 2×), 128.3 (d), 126.4 (d), 124.5 (d), 38.7 (t), 33.6 (s), 27.9 (q, 2×), 21.0 (q) ppm. MS (EI^+): m/z (%) 276 (M^+, 100), 261 (34), 234 (10), 234 (21), 233 (49), 233 (55), 218 (27), 217 (15), 215 (18), 203 (13), 204 (19). HRMS (EI^+): Calcd for $C_{20}H_{20}O$, 276.1514; found, 276.1507. IR (NaCl): ν 3024 (w, C–H), 1696 (s, C=O) cm^{-1}. UV (MeOH): λ_{max} 247 nm.

5.10. 7,8-Dihydro-8,8-dimethyl-5-(2-phenylethynyl)-naphthalene-2-carbaldehyde (20c)

Following the general procedure, the reaction of **19c** (0.3 g, 0.89 mmol), *t*-BuLi (1.0 mL, 1.7 M in pentane, 1.78 mmol) and

DMF (0.20 mL, 2.67 mmol) in THF (13 mL) afforded, after purification by chromatography (silica gel, 95:5 hexane/AcOEt), 0.18 g (71%) of a white solid identified as **20c**. Mp: 87 °C (Et_2O/hexane). Elemental Anal. Calcd for $C_{21}H_{18}O$: C, 88.08; H, 6.34. Found: C, 87.64; H, 6.33. ^1H NMR (400.16 MHz, $CDCl_3$): δ 10.02 (s, 1H), 7.89 (d, J = 7.7 Hz, 1H), 7.87 (s, 1H), 7.78 (dd, J = 7.8, 1.5 Hz, 1H), 7.6–7.4 (m, 5H), 6.67 (t, J= 4.8 Hz, 1H), 2.45 (d, J = 4.8 Hz, 2H), 1.38 (s, 6H) ppm. ^{13}C NMR (100.62 MHz, $CDCl_3$): δ 192.0 (d), 144.6 (s), 137.8 (d), 137.2 (s), 136.0 (s), 131.6 (d, 2×), 128.9 (d), 128.4 (d, 3×), 126.3 (d), 124.5 (d), 123.0 (s), 121.1 (s), 91.0 (s), 86.5 (s), 39.0 (t), 33.5 (s), 28.4 (q, 2×) ppm. MS (EI^+): m/z (%) 286 (M^+, 100), 272 (13), 271 (60), 244 (11), 243 (30), 243 (18), 242 (16), 241 (18), 239 (19), 229 (11), 228 (35), 115 (13) 91 (11). HRMS (EI^+): Calcd for $C_{21}H_{18}O$, 286.1358; found, 286.1357. IR (NaCl): ν 3053 (w, C–H), 1698 (s, C=O) cm^{-1}. UV (MeOH): λ_{max} 234, 277 nm.

5.11. 1-(7,8-Dihydro-8,8-dimethyl-5-phenyl-naphthalen-2-yl)-ethan-2-ol (21a)

5.11.1. General procedure for the synthesis of alcohols by the addition of MeLi to aldehydes

To a solution of **20a** (0.1 g, 0.38 mmol) in THF (6 mL) was added MeLi (0.26 mL, 1.6 M in Et_2O, 0.42 mmol) and the mixture was stirred for 2 h. An aqueous saturated NH_4Cl solution was added, the reaction was extracted with Et_2O (3×), the combined organic layers were dried (Na_2SO_4) and the solvent was removed. The residue was purified by chromatography (silicagel, 80:17:3 hexane/AcOEt/Et_3N), to afford 0.081 g (77%) of a white solid identified as **21a**. Mp: 80 °C (Et_2O/hexane). ^1H NMR (400.16 MHz, $CDCl_3$): δ 7.44 (dd, J = 8.3, 1.3 Hz, 1H), 7.4–7.3 (m, 6H), 7.06 (s, 1H), 6.03 (t, J = 4.6 Hz, 1H), 4.77 (q, J = 6.4 Hz, 1H), 2.38 (d, J = 4.6 Hz, 2H), 1.43 (d, J = 6.5 Hz, 3H), 1.38 (s, 3H), 1.37 (s, 3H) ppm. ^{13}C NMR (100.62 MHz, $CDCl_3$): δ 144.5 (s), 143.2 (s), 140.9 (s), 139.3 (s), 133.9 (s), 128.6 (d, 2×), 128.3 (d, 2×), 128.1 (d), 126.8 (d), 124.4 (d), 124.0 (d), 123.4 (d), 70.3 (d), 38.9 (t), 33.5 (s), 28.2 (q), 28.2 (q), 24.9 (q) ppm. MS (EI^+): m/z (%) 278 (M^+, 22), 260 (21), 245 (66), 230 (17), 219 (100), 217 (14), 215 (21), 204 (23), 203 (17), 202 (21), 85 (11), 84 (18). HRMS (EI^+): Calcd for $C_{20}H_{22}O$, 278.1671; found, 278.1676. IR (NaCl): ν 3060 (w, OH) cm^{-1}. UV (MeOH): λ_{max} 276 nm.

5.12. 1-(7,8-Dihydro-8,8-dimethyl-5-*p*-tolyl-naphthalen-2-yl)-ethan-2-ol (21b)

Following the general procedure, the reaction of **20b** (0.14 g, 0.51 mmol) and MeLi (0.35 mL, 1.6 M in Et_2O, 0.56 mmol) in THF (8 mL) afforded, after purification by chromatography (silica gel, 80:17:3 hexane/AcOEt/Et_3N), 0.13 g (88%) of a yellow oil identified as **21b**. ^1H NMR (400.16 MHz, $CDCl_3$): δ 7.29 (d, J = 1.4 Hz, 1H), 7.2–7.1 (m, 4H), 7.02 (dd, J = 7.9, 1.5 Hz, 1H), 6.94 (d, J = 7.9 Hz, 1H), 5.86 (t, J = 4.7 Hz, 1H), 4.81 (q, J = 6.4 Hz, 1H), 2.32 (s, 3H), 2.26 (d, J = 4.7 Hz, 2H), 1.43 (d, J = 6.4 Hz, 3H), 1.30 (s, 6H) ppm. ^{13}C NMR (100.62 MHz, $CDCl_3$): δ 154.4 (s), 144.8 (s), 138.9 (s), 137.9 (s), 136.6 (s), 133.2 (s), 128.8 (d, 2×), 128.4 (d, 2×), 126.1 (d), 125.7 (d), 122.5 (d), 120.8 (d), 70.5 (d), 38.8 (t), 33.7 (s), 28.1 (q, 2×), 24.9 (q), 21.1 (q) ppm. MS (EI^+): m/z (%) 292 (M^+, 23), 274 (85), 259 (100), 244 (33), 233 (43), 232 (20), 231 (79), 229 (35), 215 (31), 202 (26), 81 (24), 69 (49), 67 (12). HRMS (EI^+): Calcd for $C_{21}H_{24}O$, 292.1827; found, 292.1833. IR (NaCl): ν 3030 (w, OH) cm^{-1}. UV (MeOH): λ_{max} 272 nm.

5.13. 1-[7,8-Dihydro-8,8-dimethyl-5-(2-phenylethynyl)-naphthalen-2-yl]-ethan-1-ol (21c)

Following the general procedure, the reaction of **20c** (0.12 g, 0.42 mmol) and MeLi (0.3 mL, 1.6 M in Et_2O, 0.46 mmol) in THF (7 mL) afforded, after purification by chromatography (silica gel, 80:17:3 hexane/AcOEt/Et_3N), 0.10 g (83%) of a yellow oil identified as **21c**. ^1H NMR (400.16 MHz, $CDCl_3$): δ 7.71 (d, J = 7.9 Hz, 1H), 7.55 (dd, J = 7.9, 2.6 Hz, 1H), 7.5–7.2 (m, 6H), 6.49 (t, J = 4.9 Hz, 1H), 4.93 (q, J = 6.3 Hz), 2.66 (d, J = 6.7 Hz, 3H), 2.39 (d, J = 4.9 Hz, 2H), 1.33 (s, 6H) ppm. ^{13}C NMR (100.62 MHz, $(CD_3)_2CO$): δ 147.2 (s), 144.0 (s), 136.2 (d), 133.2 (d, 2×), 132.7 (s), 130.5 (d, 2×), 130.2 (s), 127.4 (d), 125.4 (d), 125.3 (d), 124.6 (d), 123.4 (s), 92.1 (s), 89.3 (s), 70.3 (d), 40.8 (t), 34.8 (s), 27.2 (q, 2×), 27.0 (q) ppm. MS (EI^+): m/z (%) 302 (M^+, 19), 287 (18), 286 (18), 285 (22), 284 (72), 271 (23), 270 (26), 269 (100), 254 (49), 241 (70), 239 (55), 228 (28), 86 (34). HRMS (EI^+): Calcd for $C_{22}H_{22}O$, 302.1671; found, 302.1670. IR (NaCl): ν 3462 (br, OH), 2966 (s, C–H) cm^{-1}. UV (MeOH): λ_{max} 252, 323 nm.

5.14. 1-(7,8-Dihydro-8,8-dimethyl-5-phenyl-naphthalen-2-yl)-ethan-1-one (22a)

5.14.1. General procedure for the oxidation of benzylic alcohols

To a solution of **21a** (0.071 g, 0.26 mmol) in CH_2Cl_2 (2 mL) were sequentially added MnO_2 (0.49 g, 4.68 mmol) and Na_2CO_3 (0.40 g, 4.68 mmol) and the reaction was stirred for 2 h. The mixture was filtered through Celite® and the solvent was removed. The residue was purified by chromatography (silicagel, 90:7:3 hexane/AcOEt/Et_3N) to afford 0.071 g (99%) of a white solid identified as **22a**. Mp: 71 °C (Et_2O/hexane). Elemental Anal. Calcd for $C_{20}H_{20}O$: C, 86.92; H, 7.28. Found: C, 86.64; H, 7.26. ^1H NMR (400.16 MHz, $CDCl_3$): δ 7.85 (dd, J = 8.1, 1.7 Hz, 1H), 7.65 (d, J = 1.5 Hz, 1H), 7.47 (d, J = 8.1 Hz, 1H), 7.4–7.3 (m, 5H), 6.06 (t, J = 4.6 Hz, 1H), 2.46 (s, 3H), 2.40 (d, J = 4.7 Hz, 2H), 1.38 (s, 6H) ppm. ^{13}C NMR (100.62 MHz, $CDCl_3$): δ 197.8 (s), 150.6 (s), 140.2 (s), 138.9 (s), 134.9 (s), 134.0 (s), 128.4 (d, 2×), 128.3 (d, 2×), 127.5 (d), 127.3 (d), 127.1 (d), 125.7 (d), 123.9 (d), 38.5 (t), 33.9 (s), 27.8 (q), 26.4 (q, 2×) ppm. MS (EI^+): m/z (%) 276 (M^+, 100), 262 (12), 261 (53), 234 (25), 233 (50), 219 (37), 218 (20), 217 (15), 215 (18), 204 (19), 203 (33), 202 (58), 191 (23), 189 (15). HRMS (EI^+): Calcd for $C_{20}H_{20}O$, 276.1514; found, 276.1510. IR (NaCl): ν 2959 (w, C–H), 1682 (s, C=O) cm^{-1}. UV (MeOH): λ_{max} 248 nm.

5.15. 1-(7,8-Dihydro-8,8-dimethyl-5-*p*-tolyl-naphthalen-2-yl)-ethan-1-one (22b)

Following the general procedure, the reaction of **21b** (0.043 g, 0.15 mmol), MnO_2 (0.29 g, 2.7 mmol) and Na_2CO_3 (0.23 g, 2.7 mmol) in CH_2Cl_2 (2 mL) afforded, after purification by chromatography (silica gel, 90:7:3 hexane/AcOEt/Et_3N), 0.038 g (87%) of a white solid identified as **22b**. Mp: 77 °C (Et_2O/hexane). Elemental Anal. Calcd for $C_{21}H_{22}O$: C, 86.85; H, 7.64. Found: C, 86.50; H, 7.65. ^1H NMR (400.16 MHz, $CDCl_3$): δ 7.84 (dd, J = 8.1, 1.8 Hz, 1H), 7.67 (d, J = 1.8 Hz, 1H), 7.46 (d, J = 8.1 Hz, 1H), 7.3–7.2 (m, 4H), 6.04 (t, J = 4.7 Hz, 1H), 2.47 (s, 3H), 2.42 (s, 3H), 2.38 (d, J = 4.7 Hz, 2H), 1.37 (s, 6H) ppm. ^{13}C NMR (100.62 MHz, $CDCl_3$): δ 197.9 (s), 145.5 (s), 138.9 (s), 138.5 (s), 137.4 (s), 137.0 (s), 129.0 (d, 2×), 128.9 (d, 2×), 128.8 (s), 128.5 (d), 126.5 (d), 126.0 (d), 123.6 (d), 38.9 (t), 33.7 (s), 30.4 (q), 28.1 (q), 26.6 (q, 2×) ppm. MS (EI^+): m/z (%) 290 (M^+, 100), 276 (17), 275 (41), 248 (20), 247 (92), 233 (52), 232 (19), 218 (21), 217 (20), 216 (19), 115 (40), 202 (37). HRMS (EI^+): Calcd for $C_{21}H_{22}O$, 290.1671; found, 290.1670. IR (NaCl): ν 3023 (w, C–H), 1728 (s, C=O) cm^{-1}. UV (MeOH): λ_{max} 248 nm.

5.16. 1-[7,8-Dihydro-8,8-dimethyl-5-(2-phenylethynyl)-naphthalen-2-yl]-ethan-1-one (22c)

Following the general procedure, the reaction of **21c** (0.1 g, 0.37 mmol), MnO_2 (0.70 g, 6.7 mmol) and Na_2CO_3 (0.58 g,

6.7 mmol) in CH_2Cl_2 (5 mL) afforded, after purification by chromatography (silica gel, 90:7:3 hexane/AcOEt/Et_3N), 0.096 g (86%) of a white solid identified as **22c**. Mp: 75 °C (Et_2O/hexane). Elemental Anal. Calcd for $C_{22}H_{20}O$: C, 87.96; H, 6.71. Found: C, 87.74; H, 6.67. ^{1}H NMR (400.16 MHz, $CDCl_3$): δ 8.24 (d, J = 1.8 Hz, 1H), 7.80 (dd, J = 8.1, 1.9 Hz, 1H), 7.5–7.4 (m, 2H), 7.34 (d, J = 8.1 Hz, 1H), 7.3–7.2 (m, 3H), 6.47 (t, J= 4.9 Hz, 1H), 2.56 (s, 3H), 2.33 (d, J = 4.9 Hz, 2H), 1.25 (s, 6H) ppm. ^{13}C NMR (100.62 MHz, $CDCl_3$): δ 197.6 (s), 149.0 (s), 135.3 (s), 134.8 (d), 131.5 (s), 131.4 (d, 2×), 128.3 (d, 3×), 128.2 (d), 128.0 (d), 125.7 (s), 123.9 (d), 120.8 (s), 91.0 (s), 86.6 (s), 38.7 (t), 33.7 (s), 28.2 (q, 2×), 26.4 (q) ppm. MS (EI$^+$): *m/z* (%) 300 (M$^+$, 100), 286 (22), 285 (94), 257 (38), 243 (29), 242 (46), 241 (29), 240 (18), 239 (38), 226 (29). HRMS (EI$^+$): Calcd for $C_{22}H_{20}O$, 300.1514; found, 300.1517. IR (NaCl): ν 3057 (w, C–H), 1682 (s, C=O) cm^{-1}. UV (MeOH): λ_{max} 252 nm.

5.17. 4-[(1*E*)-3-(7,8-Dihydro-8,8-dimethyl-5-phenylnaphthalen-2-yl)-3-oxoprop-1-en-1-yl]-benzoic Acid (24a)

5.17.1. General procedure for the Claisen–Schmidt condensation

To a solution of **22a** (0.035 g, 0.13 mmol) in MeOH (1.5 mL) was added ethyl 4-formylbenzoate **23** (0.020 g, 0.13 mmol) and a 1 N aqueous NaOH solution (0.8 mL). After stirring for 15 h, the solvent was removed and a 10% aqueous HCl solution was added until acidic pH. The mixture was extracted with CH_2Cl_2 (3×), the combined organic layers were dried (Na_2SO_4) and the solvent was removed. The residue was purified by chromatography (silicagel, 95:5 CH_2Cl_2/MeOH) to afford 0.034 g (63%) of a white solid identified as **24a**. Mp: 106 °C (acetone/hexane). ^{1}H NMR (400.16 MHz, $(CD_3)_2CO$): δ 8.17 (s, 1H), 8.11 (d, J = 8.2 Hz, 2H), 8.01 (d, J = 15.7 Hz, 1H), 7.96 (d, J = 8.0 Hz, 2H), 7.84 (d, J = 15.7 Hz, 1H), 7.5–7.4 (m, 6H), 7.13 (d, J = 8.0 Hz, 1H), 6.19 (t, J = 4.7 Hz, 1H), 2.46 (d, J = 4.7 Hz, 2H), 1.43 (s, 6H) ppm. ^{13}C NMR (100.62 MHz, $(CD_3)_2CO$): δ 190.2 (s), 167.3 (s), 147.5 (s), 144.0 (d), 142.2 (s), 141.0 (s), 140.0 (s), 138.9 (s), 133.3 (d, 2×), 131.9 (d), 131.2 (d), 130.9 (d), 130.5 (s), 130.4 (d, 2×), 130.3 (d, 2×), 129.3 (d), 129.2 (s), 128.5 (d), 127.8 (d), 127.7 (d), 126.9 (d), 40.4 (t), 35.4 (s), 29.3 (q, 2×) ppm. MS (EI$^+$): *m/z* (%) 408 (M$^+$, 89), 407 (10), 394 (12), 393 (35), 379 (12), 366 (21), 365 (19), 202 (16), 180 (29), 175 (68), 131 (12), 131 (48), 118 (31), 103 (24). HRMS (EI$^+$): Calcd for $C_{28}H_{24}O_3$, 408.1725; found, 408.1718. IR (NaCl): ν 3028 (br, OH), 1687 (s, C=O), 1606 (s, C=O) cm^{-1}. UV (MeOH): λ_{max} 319 nm.

5.18. 4-[(1*E*)-3-(7,8-Dihydro-8,8-dimethyl-5-*p*-tolylnaphthalen-2-yl)-3-oxoprop-1-en-1-yl]-benzoic Acid (24b)

Following the general procedure, the reaction of **22b** (0.038 g, 0.13 mmol), ethyl 4-formylbenzoate **23** (0.021 g, 0.13 mmol) and a 1 N aqueous NaOH solution (1 mL) in MeOH (2 mL) afforded, after purification by chromatography (silica gel, 95:5 CH_2Cl_2/MeOH), 0.040 g (72%) of a yellow solid identified as **24b**. Mp: 115 °C (AcOEt/hexane). Elemental Anal. Calcd for $C_{29}H_{26}O_3{\cdot}H_2O$: C, 79.07; H, 6.41. Found: C, 78.60; H, 5.99. ^{1}H NMR (400.16 MHz, $(CD_3)_2CO$): δ 8.19 (s, 1H), 8.15 (d, J = 8.1 Hz), 8.1–7.9 (m, 5H), 7.88 (d, J = 15.7 Hz, 1H·), 7.3–7.2 (m, 4H), 7.19 (d, J = 8.1 Hz, 1H), 6.19 (t, J = 4.6 Hz, 1H), 2.48 (d, J = 4.5 Hz, 2H), 2.43 (s, 3H), 1.46 (s, 6H) ppm. ^{13}C NMR (100.62 MHz, $(CD_3)_2CO$): δ 190.2 (s), 171.8 (s), 147.5 (s), 144.1 (d), 140.9 (s), 140.1 (s), 139.2 (s), 138.8 (s), 131.9 (d), 131.3 (d), 131.2 (d), 131.2 (s), 130.9 (d, 2×), 130.7 (d), 130.4 (d, 2×), 130.3 (d), 130.3 (d), 128.5 (s), 127.8 (s), 126.0 (d), 125.9 (d), 40.4 (t), 35.4 (s), 29.3 (q, 2×), 22.2 (q) ppm. MS (EI$^+$): *m/z* (%) 422 (M$^+$, 100), 408 (16), 407 (35), 380 (25), 379 (40), 360 (19), 318 (15), 317 (45), 247 (11), 215 (14), 202 (11), 175 (49), 103 (19). HRMS (EI$^+$): Calcd for $C_{29}H_{26}O_3$, 422.1882; found, 422.1897. IR (NaCl): ν 3017 (br, OH), 1683 (s, C=O), 1606 (s, C=O) cm^{-1}. UV (MeOH): λ_{max} 318 nm.

5.19. 4-[(1*E*)-3-(7,8-Dihydro-8,8-dimethyl-5-(2-phenylethynyl)-naphthalen-2-yl)-3-oxoprop-1-en-1-yl]-benzoic Acid (24c)

Following the general procedure, the reaction of **22c** (0.050 g, 0.17 mmol), ethyl 4-formylbenzoate 23 (0.030 g, 0.17 mmol) and a 1 N aqueous NaOH solution (1 mL) in MeOH (1.5 mL) afforded, after purification by chromatography (silicagel, 95:5 CH_2Cl_2/MeOH), 0.057 g (78%) of a yellow solid identified as **24c**. Mp: 117 °C (AcOEt/hexane). Elemental Anal. Calcd for $C_{30}H_{24}O_3{\cdot}H_2O$: C, 79.90; H, 5.82. Found: C, 80.00; H, 5.50. ^{1}H NMR (400.16 MHz, $(CD_3)_2CO$): δ 8.1–8.0 (m, 3H), 7.96 (d, J = 8.2 Hz, 2H), 7.89 (d, J = 15.7 Hz, 1H), 7.83 (d, J = 8.2 Hz, 2H), 7.76 (d, J = 8.5 Hz, 2H), 7.71 (d, J = 15.6 Hz, 1H), 7.5–7.2 (m, 3H), 6.55 (t, J = 4.8 Hz, 1H), 2.36 (d, J = 4.8 Hz, 2H), 1.25 (s, 6H) ppm. ^{13}C NMR (100.62 MHz, $(CD_3)_2CO$): δ 190.3 (s), 168.1 (s), 146.2 (s), 144.2 (d), 141.3 (s), 139.6 (s), 139.4 (d), 137.4 (s), 133.3 (d, 2×), 131.9 (d), 131.3 (d), 131.2 (d), 130.5 (d, 2×), 130.5 (d), 130.4 (d), 129.0 (d), 127.6 (d), 126.2 (d), 125.9 (d), 124.9 (s), 122.7 (s), 92.6 (s), 88.3 (s), 40.6 (t), 35.2 (s), 29.6 (q, 2×) ppm. MS (EI$^+$): *m/z* (%) 432 (M$^+$, 100), 422 (10), 418 (19), 417 (60), 408 (24), 390 (14), 389 (13), 257 (11), 175 (53), 103 (21). HRMS (EI$^+$): Calcd for $C_{30}H_{24}O_3$, 432.1725; found, 432.1727. IR (NaCl): ν 3431 (br, OH), 1690 (s, C=O), 1606 (s, C=O) cm^{-1}. UV (MeOH): λ_{max} 299 nm.

5.20. *rac*-4-[(1*E*)-3-(7,8-Dihydro-8,8-dimethyl-5-phenylnaphthalen2-yl)-3-hydroxy-prop-1-en-1-yl]-benzoic Acid (25a)

5.20.1. General procedure for the Luche reduction

A solution of **24a** (0.062 g, 0.15 mmol) and $CeCl_3{\cdot}7H_2O$ (0.051 g, 0.19 mmol) in MeOH (3 mL) was treated at 0 °C with $NaBH_4$ (0.006 g, 0.15 mmol) for 1 h. A 10% aqueous HCl solution was added, the mixture was extracted with CH_2Cl_2, the combined organic layers were dried with Na_2SO_4 and the solvent was removed. Purification by column chromatography (silica gel, 90:10 CH_2Cl_2/MeOH) afforded 0.050 g (81%) of a white solid identified as **25a**. Mp: 107 °C (AcOEt/hexane). Elemental Anal. Calcd for $C_{28}H_{26}O_3$: C, 81.92; H, 6.38. Found: C, 82.34; H, 6.73. ^{1}H NMR (400.16 MHz, $(CD_3)_2CO$): δ 8.21 (s, 1H), 8.17 (d, J = 8.1 Hz), 8.1–7.8 (m, 6H), 7.82 (d, J = 15.6 Hz, 1H), 7.3–7.2 (m, 4H), 7.17 (d, J = 8.1 Hz, 1H), 6.21 (t, J = 4.5 Hz, 1H), 5.20 (s, 1H), 2.43 (d, J = 4.5 Hz, 2H), 2.41 (s, 3H), 1.43 (s, 6H) ppm. ^{13}C NMR (100.62 MHz, $(CD_3)_2CO$): δ 167.3 (s), 147.5 (s), 144.1 (d), 142.1 (s), 140.1 (s), 140.0 (s), 138.9 (s), 131.9 (d, 2×), 131.2 (d), 130.9 (d), 130.5 (s), 130.9 (s), 130.4 (d), 130.3 (d, 2×), 129.2 (d), 129.2 (d), 128.6 (d), 127.8 (d), 126.9 (d), 126.2 (d), 125.9 (d), 73.1 (d), 40.4 (t), 34.5 (s), 30.1 (q, 2×), 23.2 (q) ppm. MS (EI$^+$): *m/z* (%) 410 (M$^+$, 100), 409 (10), 408 (16), 406 (31), 380 (25), 379 (40), 360 (19), 318 (15), 317 (40), 247 (11), 215 (14), 202 (11), 175 (49), 103 (21). HRMS (EI$^+$): Calcd for $C_{28}H_{26}O_3$, 410.1920; found, 410.2002. IR (NaCl): ν 3017 (br, OH), 1683 (s, C=O), 1606 (s, C=O) cm^{-1}. UV (MeOH): λ_{max} 277 nm.

5.21. *rac*-4-[(1*E*)-3-(7,8-Dihydro-8,8-dimethyl-5-p-tolylnaphthalen-2-yl)-3-hydroxy-prop-1-en-1-yl]-benzoic Acid (25b)

Following the general procedure, the reaction of **24b** (0.040 g, 0.094 mmol) with $CeCl_3{\cdot}7H_2O$ (0.033 g, 0.12 mmol) and $NaBH_4$ (0.003 g, 0.094 mmol) in MeOH (2 mL) afforded, after purification by column chromatography (silica gel, 90:10 CH_2Cl_2/MeOH), 0.037 g (92%) of a yellow solid identified as **25b**. Mp: 110 °C (AcOEt/hexane). Elemental Anal. Calcd for $C_{29}H_{28}O_3$: C, 82.05; H, 6.65. Found: C, 82.34; H, 6.73. ^{1}H NMR (400.16 MHz, $(CD_3)_2CO$): δ 8.21 (s, 1H), 8.17 (d, J = 8.1 Hz·), 8.1–7.9 (m, 5H), 7.9 (d, J = 15.6 Hz, 1H), 7.31 (s, 4H), 7.23 (d, J = 8.2 Hz, 1H), 6.21 (t, J = 4.6 Hz, 1H), 5.32 (s, 1H), 2.48 (d, J = 4.5 Hz, 2H), 2.42 (s, 3H), 1.43 (s, 6H) ppm. ^{13}C NMR (100.62 MHz, $(CD_3)_2CO$): δ 168.1 (s),

152.6 (s), 143.9 (d), 141.3 (s), 140.8 (s), 139.4 (s), 138.8 (s), 137.7 (s), 136.3 (s), 133.7 (s), 131.9 (d, 2×), 131.3 (d, 2×), 130.9 (d), 130.3 (d, 2×), 130.1 (d), 128.7 (d), 128.6 (d), 127.6 (d), 126.5 (d), 126.1 (d), 72.1 (d), 40.4 (t), 35.7 (s), 29.2 (q, 2×), 22.2 (q) ppm. MS (EI^+): *m/z* (%) 424 (M^+, 100), 423 (32), 422 (20), 408 (16), 406 (31), 380 (25), 379 (40), 360 (19), 318 (15), 317 (40), 247 (11), 215 (14), 202 (11), 175 (49), 103 (21). HRMS (EI^+): Calcd for $C_{29}H_{28}O_3$, 424.2002; found, 424.2003. IR (NaCl): *ν* 3017 (br, OH), 1683 (s, C=O), 1606 (s, C=O) cm^{-1}. UV (MeOH): λ_{max} 267 nm.

5.22. *rac*-4-[(1*E*)-3-(7,8-Dihydro-8,8-dimethyl-5-(2-phenylethynyl)-naphthalen-2-yl)-3-hydroxyprop-1-enyl]benzoic Acid (25c)

Following the general procedure, the reaction of **24c** (0.040 g, 0.093 mmol) with $CeCl_3{\cdot}7H_2O$ (0.033 g, 0.12 mmol) and $NaBH_4$ (0.003 g, 0.094 mmol) in MeOH (2 mL) afforded, after purification by column chromatography (silica gel, 90:10 CH_2Cl_2/MeOH), 0.036 g (90%) of a yellow solid identified as **25c**. M. p.: 109 °C (AcOEt/hexane). Elemental Anal. Calcd for $C_{29}H_{28}O_3$: C, 82.05; H, 6.65. Found: C, 82.34; H, 6.73. ^1H NMR (400.16 MHz, $(CD_3)_2CO$): *δ* 8.1–7.9 (m, 3H), 7.98 (d, *J* = 8.1 Hz, 2H), 7.90 (d, *J* = 15.5 Hz, 1H), 7.82 (d, *J* = 8.2 Hz, 2H), 7.73 (d, *J* = 8.5 Hz, 2H), 7.69 (d, *J* = 15.6 Hz, 1H), 7.5–7.2 (m, 3H), 6.49 (t, *J* = 4.8 Hz, 1H), 5.20 (s, 1H), 2.36 (d, *J* = 4.9 Hz, 2H), 1.23 (s, 6H) ppm. ^{13}C NMR (100.62 MHz, $(CD_3)_2CO$): *δ* 168.1 (s), 146.2 (s), 144.2 (d), 141.3 (s), 139.6 (s), 139.4 (d), 133.3 (d, 2×), 132.0 (d, 2×), 131.3 (s), 131.2 (d), 130.5 (d, 2×), 130.5 (d), 130.4 (s), 129.0 (d), 127.6 (d), 126.2 (d), 125.9 (d), 125.0 (s), 122.7 (s), 91.4 (s), 87.2 (s), 73.1 (d), 40.6 (t), 34.3(s), 28.9 (q, 2×) ppm. MS (EI^+): *m/z* (%) 434 (M^+, 100), 422 (10), 418 (19), 417 (60), 408 (24), 390 (14), 389 (13), 257 (11), 175 (53), 103 (21). HRMS (EI^+): Calcd for $C_{30}H_{26}O_3$, 434.1925; found, 434.1927. IR (NaCl): *ν* 3431 (br, OH), 1690 (s, C=O), 1606 (s, C=O) cm^{-1}. UV (MeOH): λ_{max} 299 nm.

5.23. *rac*-4-[(3-(8,8-Dimethyl-5-phenyl-7,8-dihydronaphthalen-2-yl)-4,5-dihydroisoxazol-5-yl)]benzoic Acid (26a)

5.23.1. General procedure for the addition of hydroxylamine to chalcones

To a solution of $NH_2OH{\cdot}HCl$ (0.07 g, 0.085 mmol) and NaOAc (0.01 g, 0.13 mmol) in MeOH (0.2 mL) was added a solution of **24a** (0.035 g, 0.09 mmol) in MeOH (0.5 mL) and the mixture was heated to 70 °C for 16 h. The solvent was removed and brine was added. The mixture was then extracted with CH_2Cl_2 (3×), the combined organic layers were dried (Na_2SO_4) and the solvent was removed. The residue was purified by chromatography (silica gel, 90:10 CH_2Cl_2/MeOH), to afford 0.027 g (75%) of a white solid identified as **26a**. M. p.: 115 °C (acetone/hexane). ^1H NMR (400.16 MHz, $(CD_3)_2CO$): *δ* 8.19 (s, 1H), 8.15 (d, *J* = 8.3 Hz, 2H), 7.97 (d, *J* = 8.0 Hz, 2H), 7.4–7.3 (m, 6H), 7.13 (d, *J* = 8.0 Hz, 1H), 6.19 (t, *J* = 4.5 Hz, 1H), 5.93 (t, *J* = 3.6 Hz, 1H), 3.9–3.6 (m, 2H), 2.45 (d, *J* = 4.6 Hz, 2H), 1.41 (s, 6H) ppm. ^{13}C NMR (100.62 MHz, $(CD_3)_2CO$): *δ* 189.1 (s), 167.3 (s), 156.2 (s), 147.5 (s), 144.0 (d), 142.2 (s), 141.0 (s), 139.2 (s), 138.9 (s), 133.3 (d, 2×), 131.9 (d), 131.2 (d), 130.9 (d), 130.5 (s), 130.4 (d, 2×), 130.3 (d, 2×), 129.3 (d), 129.2 (s), 128.5 (d), 127.8 (d), 127.7 (d), 126.9 (d), 80.9 (s), 42.0 (d), 40.3 (t), 35.4 (s), 29.3 (q, 2×) ppm. MS (EI^+): *m/z* (%) 423 (M^+, 100), 407 (10), 394 (12), 393 (35), 180 (29), 175 (68), 131 (48), 118 (31), 103 (24). HRMS (EI^+): Calcd for $C_{28}H_{25}NO_3$, 423.1725; found, 423.1719. IR (NaCl): *ν* 3030 (br, OH), 1685 (s, C=O), 1616 (s, C=O) cm^{-1}. UV (MeOH): λ_{max} 257 nm.

5.24. *rac*-4-[(3-(8,8-Dimethyl-5-*p*-tolyl-7,8-dihydronaphthalen-2-yl)-4,5-dihydroisoxazol-5-yl)]benzoic Acid (26b)

Following the general procedure, the reaction of **24b** (0.051 g, 0.12 mmol) with $NH_2OH{\cdot}HCl$ (0.009 g, 0.14 mmol) and NaOAc (0.02 g, 0.21 mmol) in MeOH (2 mL) afforded, after purification by column chromatography (silica gel, 90:10 CH_2Cl_2/MeOH), 0.048 g (93%) of a yellow solid identified as **26b**. Mp: 113 °C (AcOEt/hexane). ^1H NMR (400.16 MHz, $(CD_3)_2CO$): *δ* 8.20 (s, 1H), 8.16 (d, *J* = 8.1 Hz), 8.1–7.8 (m, 4H), 7.31 (s, 4H), 7.23 (d, *J* = 8.1 Hz, 1H), 6.22 (t, *J* = 4.5 Hz, 1H), 5.03 (t, *J* = 4.5 Hz, 1H), 3.85 (m, 1H), 3.60 (m, 1H), 2.48 (d, *J* = 4.5 Hz, 2H), 2.42 (s, 3H), 1.45 (s, 6H) ppm. ^{13}C NMR (100.62 MHz, $(CD_3)_2CO$): *δ* 169.3 (s), 156.2 (s), 151.9 (s), 139.4 (s), 139.2 (s), 137.0 (s), 137.6 (s), 135.2 (s), 133.8 (s), 132.5 (s), 130.4 (d, 2×), 129.7 (d), 129.1 (d, 2×), 128.9 (d, 2×), 126.3 (d, 2×), 126.2 (d), 124.9 (d), 123.9 (d), 80.9 (d), 48.4 (s), 45.9 (t), 42.0 (t), 29.2 (q, 2×), 24.3 (q) ppm. MS (EI^+): *m/z* (%) 437 (M^+, 100), 423 (32), 422 (20), 408 (16), 406 (31), 380 (25), 379 (40), 360 (19), 318 (15), 317 (40), 247 (11), 215 (14), 202 (11), 175 (49), 103 (21). HRMS (EI^+): Calcd for $C_{29}H_{27}NO_3$, 437.2102; found, 437.2103. IR (NaCl): *ν* 3007 (br, OH), 1693 (s, C=O), 1616 (s, C=O) cm^{-1}. UV (MeOH): λ_{max} 260 nm.

5.25. *rac*-4-[3-(8,8-Dimethyl-5-(phenylethynyl)-7,8-dihydronaphthalen-2-yl)-4,5-dihydroisoxazol-5-yl]benzoic Acid (26c)

Following the general procedure, the reaction of **24c** (0.040 g, 0.08 mmol) with $NH_2OH{\cdot}HCl$ (0.007 g, 0.096 mmol) and NaOAc (0.02 g, 0.14 mmol) in MeOH (1 mL) afforded, after purification by column chromatography (silica gel, 90:10 CH_2Cl_2/MeOH), 0.020 g (93%) of a yellow solid identified as **26c**. Mp: 113 °C (AcOEt/hexane). ^1H NMR (400.16 MHz, $(CD_3)_2CO$): *δ* 8.1–7.9 (m, 3H), 7.98 (d, *J* = 8.1 Hz, 2H), 7.75 (d, *J* = 8.2 Hz, 2H), 7.73 (d, *J* = 8.5 Hz, 2H), 7.5–7.2 (m, 3H), 6.49 (t, *J* = 4.8 Hz, 1H), 5.12 (t, *J* = 4.6 Hz, 1H), 3.91 (m, 1H), 3.71 (m, 1H), 2.50 (d, *J* = 4.7 Hz, 2H·), 1.23 (s, 6H) ppm. ^{13}C NMR (100.62 MHz, $(CD_3)_2CO$): *δ* 169.3 (s), 156.2 (s), 151.9 (s), 141.3 (s), 139.6 (s), 133.5 (s), 133.3 (d, 2×), 131.4 (d, 2×), 128.5 (d, 3×), 128.3 (d), 127.0 (s), 126.2 (s), 124.9 (d), 123.9 (d), 122.7 (s), 93.1 (s), 89.2 (s), 80.9 (d), 47.5 (s), 45.1 (t), 42.0 (t), 29.2 (q, 2×) ppm. MS (EI^+): *m/z* (%) 447 (M^+, 100), 422 (10), 418 (19), 417 (60), 408 (24), 390 (14), 389 (13), 257 (11), 175 (53), 103 (21). HRMS (EI^+): Calcd for $C_{30}H_{25}NO_3$, 447.1915; found, 434.1927. IR (NaCl): *ν* 3431 (br, OH), 1690 (s, C=O), 1606 (s, C=O) cm^{-1}. UV (MeOH): λ_{max} 244 nm.

5.26. Methyl 2-(7,8-Dihydro-8,8-dimethyl-5-phenylnaphthalen-2-yl)-2-oxoacetate (27a)

5.26.1. General procedure for the synthesis of α-ketoesters

To a solution of **19a** (0.25 g, 0.79 mmol) in THF (5 mL) at − 78 °C was added *t*-BuLi (1 mL, 1.7 M in pentane, 1.7 mmol). After 30 min, a solution of dimethyloxalate (0.93 g, 7.9 mmol) in THF (6 mL) was added and the mixture was stirred for 30 min at −78 °C and for 4 h at 25 °C. The mixture was treated with a saturated aqueous solution of NH_4Cl, and extracted with Et_2O (3×). The combined organic layers were washed with H_2O, dried (Na_2SO_4) and the solvent was removed. The residue was purified by chromatography (silicagel, 95:5 hexane/AcOEt), to afford 0.19 g (75%) of a yellow oil identified as **27a**. ^1H NMR (400.16 MHz, $CDCl_3$): *δ* 8.03 (d, *J* = 1.7 Hz, 1H), 7.71 (dd, *J* = 8.1, 1.7 Hz, 1H), 7.4–7.3 (m, 5H), 7.14 (d, *J* = 8.1 Hz, 1H), 6.19 (t, *J* = 4.6 Hz, 1H), 3.97 (s, 3H), 2.42 (d, *J* = 4.6 Hz, 2H), 1.41 (s, 6H) ppm. ^{13}C NMR (100.62 MHz, $CDCl_3$): *δ* 185.5 (s), 164.2 (s), 145.8 (s), 140.2 (s), 139.8 (s), 138.9 (s), 131.1 (s), 130.7 (d), 128.5 (d, 2×), 128.5 (d), 128.3 (d, 2×), 127.4 (d), 126.2 (d), 125.1 (d), 52.5 (q), 38.7 (t), 33.7 (s), 27.9 (q, 2×) ppm. MS (EI^+): *m/z* (%) 320 (M^+, 16), 309 (11), 293 (34), 281 (19), 280 (100), 278 (15), 277 (69), 275 (18), 262 (16), 261 (80), 247 (12), 233 (15), 221 (30), 215 (14), 203 (16), 202 (16), 191 (11), 189 (14), 165 (14), 115 (11), 113 (30), 105 (38), 91 (13), 86 (13), 84 (20). HRMS (EI^+): calcd for $C_{21}H_{20}O_3$, 320.1412; found, 320.1398. IR (NaCl): *ν* 2829 (m, C–H), 1737 (s, C=O), 1679 (s, C=O) cm^{-1}. UV (MeOH): λ_{max} 330 nm.

5.27. Methyl 2-(7,8-Dihydro-8,8-dimethyl-5-*p*-tolylnaphthalen-2-yl)-2-oxoacetate (27b)

Following the general procedure, the reaction of **19b** (0.25 g, 0.76 mmol), *t*-BuLi (1.3 mL, 1.7 M in pentane, 2.25 mmol) and dimethyloxalate (0.89 g, 7.6 mmol) in THF (12 mL) afforded, after purification by chromatography (silica gel, 95:5 hexane/AcOEt), 0.21 g (83%) of a yellow oil identified as **27b**. ^{1}H NMR (400.16 MHz, $CDCl_3$): δ 8.20 (s, 1H), 7.87 (dd, J = 8.1, 1.5 Hz, 1H), 7.4–7.3 (m, 4H), 7.34 (d, J = 7.9 Hz, 1H), 6.35 (t, J = 4.4 Hz, 1H), 4.15 (s, 3H), 2.58 (d, J = 4.3 Hz, 2H), 1.61 (s, 6H$_2$) ppm. ^{13}C NMR (100.62 MHz, $CDCl_3$): δ 185.6 (s), 164.3 (s), 145.8 (s), 140.3 (s), 138.8 (s), 137.1 (s), 136.9 (s), 131.0 (s), 130.3 (d), 129.0 (d), 128.5 (d, 2×), 128.4 (d, 2×), 126.2 (d), 125.1 (d), 52.5 (q), 38.7 (t), 33.7 (s), 27.9 (q, 2×), 21.1 (q) ppm. MS (EI$^+$): *m/z* (%) 334 (M$^+$, 30), 323 (10), 309 (12), 308 (15), 307 (64), 294 (45), 291 (31), 289 (28), 279 (19), 276 (23), 275 (100), 261 (19), 215 (14), 203 (11), 202 (14), 119 (39), 91 (17). HRMS (EI$^+$): calcd for $C_{22}H_{22}O_3$, 334.1569; found, 334.1581. IR (NaCl): ν 2956 (m, C–H), 1737 (s, C=O), 1685 (s, C=O) cm^{-1}. UV (MeOH): λ_{max} 267 nm.

5.28. Methyl 2-(7,8-dihydro-8,8-dimethyl-5-(2-phenylethynyl)-naphthalen-2-yl)-2-oxoacetate (27c)

Following the general procedure, the reaction of **19c** (0.25 g, 0.74 mmol) with *t*-BuLi (0.96 mL, 1.7 M in pentane, 1.63 mmol) and dimethyloxalate (0.87 g, 7.4 mmol) in THF (11 mL) afforded, after purification by chromatography (silica gel, 95:5 hexane/AcOEt), 0.21 g (79%) of a yellow oil identified as **27c**. ^{1}H NMR (400.16 MHz, $CDCl_3$): δ 8.10 (d, J = 1.7 Hz, 1H), 7.79 (dd, J = 8.3, 1.7 Hz, 1H), 7.5–7.4 (m, 5H,), 7.16 (d, J = 8.5 Hz, 1H·), 6.23 (t, J = 4.6 Hz, 1H), 3.97 (s, 3H), 2.45 (d, J = 4.8 Hz, 2H), 1.40 (s, 6H) ppm. ^{13}C NMR (100.62 MHz, $CDCl_3$): δ 185.9 (s), 165.2 (s), 145.7 (s), 141.2 (s), 139.0 (s), 138.9 (s), 131.3 (s), 130.6 (d), 129.5 (d, 2×), 128.5 (d), 128.3 (d, 2×), 127.4 (d), 126.2 (d), 124.1 (d), 91.1 (s), 89.3 (s), 52.5 (q), 38.7 (t), 33.7 (s), 27.5 (q, 2×) ppm. MS (EI$^+$): *m/z* (%) 344 (M$^+$, 20), 310 (15), 290 (35), 282 (20), 280 (100), 277 (69), 261 (80), 221 (30), 113 (30), 105 (38), 90 (13), 86 (13), 84 (20). HRMS (EI$^+$): calcd for $C_{23}H_{20}O_3$, 344.1001; found, 344.1111. IR (NaCl): ν 2958 (s, C–H), 1740 (s, C=O), 1681 (s, C=O) cm^{-1}. UV (MeOH): λ_{max} 330 nm.

5.29. 4-[2-(7,8-Dihydro-8,8-dimethyl-5-phenylnaphthalen-2-yl)-2-oxoacetamido]-3-fluorobenzoic Acid (34a)

5.29.1. General procedure for the synthesis of 2-oxo-acetamidobenzoic acids

To a solution of **27a** (0.13 g, 0.42 mmol) in THF (1 mL) was added a solution of LiOH·H$_2$O (0.026 g, 0.63 mmol) in THF (3 mL) and H$_2$O (3 mL), and the reaction was stirred to 80 °C for 2 h. The mixture was diluted with H$_2$O, a 10% aqueous HCl solution was added and the mixture was extracted with AcOEt (3×). The combined organic layers were dried (Na_2SO_4) and the solvent was removed. The residue was purified by chromatography (silica gel, 95:5 CH_2Cl_2/MeOH), to afford 0.10 g (78%) of a yellow solid identified as **28a**. To a solution of **28a** (0.024 g, 0.078 mmol) in CH_2Cl_2 (1 mL) and DMF (0.12 mL) was added oxalyl chloride (0.020 mL, 0.23 mmol). After stirring for 1 h, the solvent was removed and the residue was diluted with AcOEt (1 mL) and treated with a solution of methyl 4-amino-3-fluorobenzoate **32** (0.017 g, 0.094 mmol) in AcOEt (1 mL) and Et_3N (0.033 mL, 0.23 mmol) and the mixture was stirred for 16 h at 25 °C. An aqueous saturated Na_2CO_3 solution was added and the mixture was extracted with AcOEt (3×). The combined organic layers were dried (Na_2SO_4) and the solvent was removed. The residue was purified by chromatography (silica gel, 80:20 hexane/AcOEt), to afford 0.021 g (58%) of a yellow solid identified as **33a**.

To a solution of **33a** (0.026 g, 0.057 mmol) in THF (0.5 mL) and MeOH (0.3 mL) was added a solution of LiOH·H$_2$O (0.007 g, 0.17 mmol) in THF (0.5 mL) and H$_2$O (1 mL), and the reaction was stirred for 4 h at 25 °C. The mixture was diluted with H$_2$O, a 10% aqueous HCl solution was added and then extracted with AcOEt (3×). The combined organic layers were dried (Na_2SO_4) and the solvent was removed. The residue was purified by chromatography (silica gel, 95:5 CH_2Cl_2/MeOH), to afford 0.10 g (78%) of a yellow solid identified as **34a**. ^{1}H NMR (400.16 MHz, $(CD_3)_2CO$): δ 9.89 (s, 1H), 8.52 (d, J = 7.9 Hz, 1H), 8.32 (s, 1H), 8.07 (d, J = 9.0 Hz, 1H), 7.94 (d, J = 7.9 Hz, 1H), 7.83 (d, $^3J_{H-F}$ = 11.3 Hz, 1H), 7.5–7.4 (m, 5H), 7.15 (d, J = 8.5 Hz, 1H), 6.26 (t, J = 4.6 Hz, 1H·), 2.49 (d, J = 4.7 Hz, 2H), 1.48 (s, 6H) ppm. ^{13}C NMR (100.62 MHz, $(CD_3)_2CO$): δ 170.1 (s), 169.3 (s), 167.5 (s), 152.3 (s, $^1J_{C-F}$ = 239.8 Hz), 147.4 (s), 145.2 (s), 138.0 (d), 132.5 (d, 2×), 131.0 (s), 130.4 (d, 2×), 129.4 (d), 128.6 (d), 128.3 (d), 127.9 (d), 127.8 (d, $^3J_{C-F}$ = 20.1 Hz), 124.9 (s), 124.5 (d), 123.8 (s), 123.1 (s), 123.2 (s), 117.9 (d, $^2J_{C-F}$ = 20.8 Hz), 40.3 (t), 35.4 (s), 29.3 (q, 2×) ppm. MS (FAB$^+$): *m/z* (%) 439 (M$^+$, 18), 438 (53), 437 (25), 422 (12), 391 (10), 307 (27), 289 (15), 166 (10), 155 (32), 154 (100). HRMS (FAB$^+$): calcd for $C_{27}H_{22}FNO_4$, 443.4701; found, 443.4711. IR (NaCl): ν 2999 (w, OH), 2923 (s, C–H), 1659 (s, C=O), 1631 (s, C=O) cm^{-1}. UV (MeOH): λ_{max} 283 nm.

5.30. 4-[2-(8,8-Dimethyl-5-*p*-tolyl-7,8-dihydronaphthalen-2-yl)-2-oxoacetamido]-3-fluorobenzoic Acid (34b)

Following the general procedure, the reaction of **27b** (0.34 g, 1.02 mmol) and LiOH·H$_2$O (0.064 g, 1.53 mmol) in THF (9 mL) and H$_2$O (8 mL) afforded, after purification by chromatography (silica gel, 95:5 CH_2Cl_2/MeOH), 0.24 g (75%) of a yellow solid identified as **28b**.

The reaction of **28b** (0.049 g, 0.15 mmol), oxalyl chloride (0.040 mL, 0.45 mmol), methyl 4-amino-3-fluorobenzoate **32** (0.033 g, 0.18 mmol) and Et_3N (0.063 mL, 0.45 mmol) in AcOEt (2 ml), CH_2Cl_2 (2 mL) and DMF (0.23 mL) afforded, after purification by chromatography (silica gel, 80:20 hexane/AcOEt), 0.045 g (64%) of a yellow solid identified as **33b**.

The reaction of **33b** (0.045 g, 0.095 mmol) and LiOH·H$_2$O (0.011 g, 0.28 mmol) in THF (1 mL), H$_2$O (1 mL) and MeOH (0.5 mL) afforded, after purification by chromatography (silica gel, 95:5 CH_2Cl_2/MeOH), 0.038 g (88%) of a white solid identified as **34b**. ^{1}H NMR (400.16 MHz, $(CD_3)_2CO$): δ 9.33 (s, 1H), 8.51 (t, J = 8.2 Hz, 1H), 8.31 (d, J = 1.7 Hz, 1H), 8.11 (dd, J = 8.2, 1.7 Hz, 1H), 7.82 (d, J = 8.3 Hz, 1H), 7.74 (dd, J = 1.6 Hz, J_{H-F} = 11.2 Hz, 1H), 7.4–7.2 (m, 4H), 7.07 (d, J = 8.2 Hz, 1H), 6.12 (t, J = 4.7 Hz, 1H), 3.63 (s, 3H), 2.35 (d, J = 4.7 Hz, 2H), 1.45 (s, 6H$_2$) ppm. ^{13}C NMR (100.62 MHz, $(CD_3)_2CO$): δ 170.7 (s), 167.3 (s), 165.8 (s), 154.8 (s, $^1J_{C-F}$ = 240.5 Hz), 144.6 (s), 139.9 (s), 137.0 (d), 132.2 (d, 2×), 133.1 (s), 130.4 (d, 2×), 130.1 (d), 129.2 (d), 128.3 (d), 125.7 (d, $^3J_{C-F}$ = 19.7 Hz), 125.1 (s), 125.0 (s), 123.9 (s), 123.8 (s), 123.1 (d), 118.0 (d, $^2J_{C-F}$ = 22.1 Hz), 115.3 (s), 53.0 (q), 40.6 (t), 44.1 (s), 28.9 (q, 2×) ppm. MS (FAB$^+$): *m/z* (%) 457 (M$^+$, 11), 327 (11), 314 (11), 307 (15), 289 (20), 285 (24), 240 (20), 228 (20), 226 (21), 167 (26), 166 (25), 165 (37), 155 (30), 154 (100). HRMS (FAB$^+$): calcd for $C_{28}H_{24}FNO_4$, 457.4901; found, 457.4910. IR (NaCl): ν 3000 (w, OH), 1702 (s, C–H), 1698 (s), 1629 (s) cm^{-1}. UV (MeOH): λ_{max} 276 nm.

5.31. 4-[2-(8,8-Dimethyl-5-(2-phenylethynyl)-7,8-dihydronaphthalen-2-yl)-2-oxoacetamido]-3-fluorobenzoic acid (34c)

Following the general procedure, the reaction of **27c** (0.14 g, 0.39 mmol) and LiOH·H$_2$O (0.025 g, 0.58 mmol) in THF (4 mL) and H$_2$O (3 mL) afforded, after purification by chromatography (silica

gel, 95:5 CH_2Cl_2/MeOH), 0.11 g (82%) of a yellow solid identified as **28c**.

The reaction of 28c (0.12 g, 0.36 mmol), oxalyl chloride (0.096 mL, 1.08 mmol), methyl 4-amino-3-fluorobenzoate **32** (0.080 g, 0.43 mmol) and Et_3N (0.15 mL, 1.08 mmol) in AcOEt (4 mL), CH_2Cl_2 (4 mL) and DMF (0.43 mL) afforded, after purification by chromatography (silica gel, 80:20 hexane/AcOEt), 0.11 g (65%) of a yellow solid identified as **33c**.

The reaction of **33c** (0.032 g, 0.066 mmol) and $LiOH·H_2O$ (0.008 g, 0.20 mmol) in THF (1 mL), H_2O (1 mL) and MeOH (0.3 mL) afforded, after purification by chromatography (silica gel, 95:5 CH_2Cl_2/MeOH), 0.025 g (81%) of a white solid identified as **34c**. ^{1}H NMR (400.16 MHz, $(CD_3)_2CO$): δ 9.89 (s, 1H), 8.52 (d, J = 7.9 Hz, 1H), 8.32 (s, 1H), 8.07 (d, J = 9.0 Hz, 1H), 7.94 (d, J = 7.9 Hz, 1H), 7.83 (d, J_{H-F}= 11.3 Hz, 1H), 7.5–7.4 (m, 5H), 7.15 (d, J = 8.5 Hz, 1H), 6.26 (t, J = 4.6 Hz, 1H), 2.49 (d, J = 4.7 Hz, 2H), 1.48 (s, 6H) ppm. ^{13}C NMR (100.62 MHz, $(CD_3)_2CO$): δ 172.7 (s), 166.3 (s), 165.8 (s), 153.8 (s, $^1J_{C-F}$ = 242.5 Hz), 145.6 (s), 139.9 (s), 136.9 (d), 133.2 (d, 2×), 133.1 (s), 130.4 (d, 2×), 130.2 (d), 128.2 (d), 128.3 (d), 125.7 (d, $^3J_{C-F}$ = 19.1 Hz), 125.1 (s), 122.9 (s), 123.1 (d), 123.0 (s), 120.4 (d), 117.8 (d, $^2J_{C-F}$ = 21.9 Hz), 115.3 (s), 92.3 (s), 88.9 (s), 40.6 (t), 43.9 (s), 29.6 (q, 2×) ppm. MS (FAB$^+$): *m/z* (%) 468 (M$^+$+1, 25), 467 (M$^+$, 53), 454 (20), 453 (40), 452 (50), 287 (68), 285 (40), 282 (44), 258 (100), 257 (38), 255 (47), 253 (32), 243 (87), 242 (46), 241 (47), 239 (56), 229 (55), 228 (54), 215 (52), 185 (39), 165 (39). HRMS (FAB$^+$): calcd for $C_{29}H_{22}FNO_4$, 467.4901; found, 467.4910. IR (NaCl): ν 2956–2850 (m), 1730 (s, C=O) cm^{-1}. UV (MeOH): λ_{max} 295, 324 nm.

5.32. *rac*-4-[2-(8,8-Dimethyl-5-phenyl-7,8-dihydronaphthalen-2-yl)-2-hydroxy-acetamido]-3-fluorobenzoic acid (36a)

5.32.1. General procedure for the synthesis of α-hydroxyacetamidobenzoic acids

To a solution of **33a** (0.012 g, 0.026 mmol) in MeOH (0.5 mL) and AcOEt (0.2 mL) was added $NaBH_4$ (0.001 g, 0.015 mmol) and the reaction was stirred for 15 min at 0 °C. A 10% aqueous HCl solution was added and the organic layer was extracted with AcOEt. The combined organic layers were washed with brine and dried (Na_2SO_4) and the solvent was removed. The residue was purified by chromatography (silicagel, 80:20 hexane/AcOEt), to afford 0.010 g (84%) of a white solid identified as **35a**. Following the general procedure for the hydrolysis of methyl esters with LiOH, the reaction of **35a** (0.010 g, 0.022 mmol) and $LiOH·H_2O$ (0.003 g, 0.066 mmol) in THF (0.5 mL), H_2O (0.5 mL) and MeOH (0.2 mL) afforded, after purification by chromatography (silica gel, 90:10 CH_2Cl_2/MeOH), 0.010 g (98%) of a white solid identified as **36a**. ^{1}H NMR (400.16 MHz, $CDCl_3$): δ 9.55 (s, 1H), 8.51 (d, J = 8.0 Hz, 1H), 7.94 (s, 1H), 8.87 (d, J = 8.2 Hz, 1H), 7.80 (d, $^3J_{H-F}$= 11.6 Hz, 1H), 7.5–7.4 (m, 6H, HPh), 6.53 (t, J = 4.5 Hz, 1H), 5.40 (s, 1H), 2.40 (d, J = 4.6 Hz, 2H), 1.30 (s, 6H) ppm. ^{13}C NMR (100.62 MHz, $(CD_3)_2CO$): δ 168.0 (s), 158.5 (s), 147.4 (s, $^1J_{C-F}$ = 241.3 Hz), 142.7 (s), 141.3 (s), 139.3 (s), 135.9 (s), 133.9 (s), 133.6 (s), 133.4 (s), 132.3 (d, 2×), 130.5 (d, 2×), 130.3 (d), 129.1 (d), 128.5 (d), 127.9 (d), 127.7 (d), 126.3 (d), 125.9 (d, $^3J_{C-F}$ = 20.0 Hz), 115.9 (d, $^2J_{C-F}$ = 21.3 Hz), 40.5 (t), 35.3 (s), 29.4 (q, 2×) ppm. MS (FAB$^+$): *m/z* (%) 446 (M$^+$+1, 100), 445 (M$^+$, 45), 437 (11), 436 (28), 318 (14), 276 (42), 154 (19). HRMS (FAB$^+$): calcd for $C_{27}H_{24}FNO_4$, 445.4811; found, 445.4810. IR (NaCl): ν 3376 (w, OH), 2960–2850 (s), 1722 (s, C=O), 1618 (m, C=O) cm^{-1}. UV (MeOH): λ_{max} 314 nm.

5.33. *rac*-4-[2-(8,8-Dimethyl-5-*p*-tolyl-7,8-dihydronaphthalen-2-yl)-2-hydroxy-acetamido]-3-fluorobenzoic Acid (36b)

Following the general procedure, the reaction of **33b** (0.015 g, 0.032 mmol) and $NaBH_4$ (0.001 g, 0.016 mmol) in MeOH (0.6 mL) and AcOEt (0.3 ml) afforded, after purification by chromatography (silica gel, 80:20 hexane/AcOEt), 0.012 g (80%) of a white solid identified as **35b**. Following the general procedure, the reaction of 35b (0.012 g, 0.022 mmol) and $LiOH·H_2O$ (0.003 g, 0.066 mmol) in THF (0.5 mL), H_2O (0.5 mL) and MeOH (0.2 mL) afforded, after purification by chromatography (silica gel, 90:10 CH_2Cl_2/MeOH), 0.010 g (98%) of a white solid identified as **36b**. ^{1}H NMR (400.16 MHz, $CDCl_3$): δ 9.65 (s, 1H), 8.63 (d, J = 8.2 Hz, 1H), 7.98 (s, 1H), 7.87 (d, J = 8.3 Hz, 1H), 7.79 (d, J_{H-F}= 11.9 Hz, 1H), 7.4–7.3 (m, 4H), 6.49 (t, J = 4.4 Hz, 1H), 5.38 (s, 1H), 2.43 (d, J = 4.6 Hz, 2H), 2.40 (s, 3H), 1.35 (s, 6H) ppm. ^{13}C NMR (100.62 MHz, $(CD_3)_2CO$): δ 172.5 (s), 167.5 (s), 155.3 (s, $^1J_{C-F}$ = 243.1 Hz), 146.6 (s), 139.7 (s), 137.7 (d, 2×), 133.2 (d), 133.1 (s), 131.3 (d, 2×), 130.5 (d), 128.2 (d), 128.1 (d), 128.0 (s), 126.7 (d, $^3J_{C-F}$ = 19.6 Hz), 125.3 (s), 122.9 (s), 122.8 (s), 122.1 (d), 116.9 (d, $^2J_{C-F}$ = 22.0 Hz), 116.3 (s), 77.4 (d), 53.4 (q), 41.5 (t), 43.9 (s), 31.1 (q, 2×) ppm. MS (FAB$^+$): *m/z* (%) 460 (M$^+$+1, 11), 459 (M$^+$, 20), (20), 285 (24), 240 (20), 228 (20), 226 (21), 215 (20), 202 (22), 189 (22), 180 (24), 167 (26), 166 (25), 165 (37), 154 (100). HRMS (FAB$^+$): calcd for $C_{28}H_{26}FNO_4$, 459.4901; found, 459.4910. IR (NaCl): ν 3450 (w, OH), 3026–2852 (m), 1719 (s, C=O), 1603 (s, C=O) cm^{-1}. UV (MeOH): λ_{max} 249, 326 nm.

5.34. *rac*-4-[2-(8,8-Dimethyl-5-(2-phenylethynyl)-7,8-dihydronaphthalen-2-yl)-2-hydroxyacetamido]-3-fluorobenzoic Acid (36c)

Following the general procedure, the reaction of **33c** (0.015 g, 0.031 mmol) and $NaBH_4$ (0.001 g, 0.016 mmol) in MeOH (0.6 mL) and AcOEt (0.3 ml) afforded, after purification by chromatography (silica gel, 80:20 hexane/AcOEt), 0.011 g (80%) of a white solid identified as **35c**. Following the general procedure, the reaction of **35c** (0.011 g, 0.022 mmol) and $LiOH·H_2O$ (0.003 g, 0.066 mmol) in THF (0.5 mL), H_2O (0.5 mL) and MeOH (0.2 mL) afforded, after purification by chromatography (silica gel, 90:10 CH_2Cl_2/MeOH), 0.010 g (91%) of a white solid identified as **36c**. ^{1}H NMR (400.16 MHz, $(CD_3)_2CO$): δ 9.54 (s, 1H), 8.50 (t, J = 8.1 Hz, 1H), 7.93 (d, J = 1.6 Hz, 1H), 7.85 (d, J = 8.7 Hz, 1H), 7.78 (d, $^3J_{H-F}$ = 11.6 Hz, 1H), 7.6–7.5 (m, 2H,), 7.4–7.3 (m, 5H), 6.51 (t, J = 4.9 Hz, 1H), 5.39 (s, 1H), 2.39 (d, J = 4.9 Hz, 2H), 1.29 (s, 6H) ppm. ^{13}C NMR (100.62 MHz, $(CD_3)_2CO$): δ 172.7 (s), 167.3 (s), 153.8 (s, $^1J_{C-F}$ = 243.5 Hz), 145.6 (s), 139.9 (s), 136.7 (d), 133.2 (d, 2×), 133.1 (s), 130.4 (d, 2×), 130.2 (d), 128.2 (d), 128.3 (d), 125.7 (d, $^3J_{C-F}$ = 18.1 Hz), 125.1 (s), 122.9 (s), 122.8 (s), 122.1 (d), 117.8 (d, $^2J_{C-F}$ = 20.9 Hz), 115.3 (s), 92.3 (s), 88.9 (s), 75.9 (d), 40.6 (t), 43.9 (s), 29.6 (q, 2×) ppm. MS (FAB$^+$): *m/z* (%) 470 (M$^+$+1, 53), 469 (M$^+$, 29), 454 (20), 453 (40), 452 (50), 287 (68), 285 (40), 282 (44), 258 (100), 257 (38), 255 (47), 243 (87), 242 (46), 241 (47), 239 (56), 229 (55), 228 (54), 215 (52). HRMS (FAB$^+$): calcd for $C_{29}H_{24}FNO_4$, 469.5001; found, 469.5010. IR (NaCl): ν 3000–2860 (w), 1660 (s), 1558 (s) cm^{-1}. UV (MeOH): λ_{max} 249, 327 nm.

5.35. Computational methods

5.35.1. Quantum mechanics calculations

The (*S*)-**26a** ligand was model-built in Insight II[49] using standard bond lengths and angles. The geometry of the ligand was then fully optimized at the DFT level with the 6-31G* basis set using the ab initio quantum chemistry program GAUSSIAN 98.[50] Charge distribution for the ligand was calculated by fitting the DFT/6-31G* electrostatic potential to atom centers using the RESP procedure[51] and van der Waals parameters for ligand atoms were transferred from those defined for related atoms in the AMBER force field (parm99).[52] Covalent and nonbonded parameters for the ligand atoms were derived, by analogy or through interpolation, from those already present in the same force field (parm99) or consistently derived, as explained in more detail elsewhere.[53]

5.35.2. Construction and refinement of human RARγ in the antagonist-bound conformation

The crystal structure of RARγ in complex with SR11254 (**4**) at 1.38 Å resolution (PDB code: 1fd0)[19] and the crystal structure of human RARα in complex with the antagonist BMS614 (**39**) at 2.50 Å resolution (PDB code: 1dkf)[39] were used to model the human RARγ in the antagonist-bound conformation in complex with (*S*)-**26a**. The ligand-binding domain of RARα shares a 70% amino acid sequence identity with LBD of RARγ, and the core structure of these two receptors has a similar overall fold. To drive the RARγ into the antagonist-bound conformation, helix H12 was manually reoriented to make it adopt the known antagonist form of RARα. A short optimization run restraining all non-H atoms in the residues to their initial coordinates then allowed readjustment of covalent bonds and van der Waals contacts without changing the overall conformation of the receptor. Then (*S*)-**26a** was positioned in the binding pocket on the basis of the crystallographic structures of the complexes of RAR with several ligands.[13,19,39–41,20,21]

5.35.3. Molecular dynamics simulations

The RARγ-(*S*)-**26a** complex was then refined using the second generation AMBER force field[52] and 3000 steps of steepest descent energy minimization and 6000 steps of conjugate gradient of only sidechain of the protein and those atoms belonging to the bound ligand. This procedure allowed readjustment of covalent bonds and van der Waals contacts without changing the overall conformation of the complex.

The molecular system was neutralized by addition of the appropriate number of sodium ions,[54] placed in positions of negative electrostatic potential and immersed in a rectangular box of ~8020 transferable intermolecular potential three point model water molecules.[55] Each water box extended 8 Å away from any solute atom, and the cutoff distance for the nonbonded interactions was 9 Å. Periodic boundary conditions were used, and electrostatic interactions were represented using the smooth particle mesh Ewald method with a grid spacing of ~1 Å. Unrestrained molecular dynamics (MD) simulations at 300 K and 1 atm were then run for 6 ns using the SANDER module in AMBER 8.[56] The constants for the temperature and pressure baths were 1.0 and 0.2 ps, respectively. SHAKE[57] was applied to all bonds involving hydrogens, and an integration step of 2 fs was used throughout. The nonbonded pair list was updated every 10 steps. The simulation protocol involving a series of progressive energy minimizations followed by a 20 ps heating phase and a 70 ps equilibration period before data collection. System coordinates were saved every 2 ps for further analysis.

5.35.4. Analysis of the molecular dynamics trajectories and electrostatic energy calculations

Three-dimensional structures and trajectories were visually inspected using the computer graphics program InsightII. Root-mean-square (rms) deviations from both, the initial structures and the average structures, interatomic distances, and snapshot geometries were obtained using the PTRAJ module in AMBER. Intermolecular van der Waals and electrostatic energies for individual residues were calculated with the ANAL module. After the equilibration period, the progression of the root-mean-square deviations (rmsd) of the coordinates of the Cα atoms with respect to the initial structure showed a notably stable behavior reflecting that the overall architecture of the protein was preserved for the whole length of the simulation. The relatively small rmsd calculated for the complex with respect to the average structure and the absence of drifting to higher rmsd values were indicative of adequate sampling during the data collection period and suggested that the simulation was long enough to capture the internal dynamics of the complex. When monitored by measuring the evolution of the rms deviation (rmsd) of (*S*)-**26a**, with respect to the initial structure, it can be clearly seen that the rmsd value of the antagonist was maintained around 0.5 Å. The simulation resulted in a stable trajectory and the relationships between secondary structures, together with the respective interactions, were also maintained, lending further support to the proposed models. All calculations were performed on the SGI R14000 Origin 3800 at CIEMAT (Madrid), on the SGI 1.5 GHz Itanium2 at CESGA (Santiago de Compostela) and locally on SGI R12000 Octane workstations.

5.36. Transient transactivation assays

Determination of RAR/RXR agonistic activity. HeLa reporter cells were stably transfected with an $(17m)_5$-βG-Luc-Neo reporter and with Gal4-mRARα (resp. β, γ) or Gal4-hRXRβ plasmids. They were maintained in DMEM that contained 5% fetal calf serum (FCS), supplemented with geneticin G418 (0.8 mg mL^{-1}), puromycin (0.3 μg mL^{-1}), hygromycin (0.2 mg mL^{-1}; added additionally only for the Gal4-hRXRβ-engineered HeLa cell line), and gentamycin (40 μg mL^{-1}). The ligand-binding assays were performed adding the ligands to the cell culture in DMEM medium without phenol red with 5% charcoal-treated FCS. To determine the RARα, RARβ, and RARγ induction potential of the ligands, equal aliquots (160,000 cells/well) of the corresponding cell line were seeded in a 24-well plate, and 12 h later the medium was replaced by a solution of the corresponding ligand in medium. The cells were incubated at 37 °C in 5% CO_2 for 12 h. After that, the cells were washed (PBS) and lysed (50 μL of lysis buffer: 25 mM Tris phosphate (pH 7.8), 2 mM EDTA, 1 mM DTT, 10% glycerol, and 1% Triton X-100) for 15 min. Equal aliquots (50 μL) of the cell lysates were transferred in an Optiplate-96, and the luminescence in RLU (relative luminescence units) was determined on a MicroLumat LB96P luminometer ('Berthold') after automatic injection of 50 μL of luciferin buffer (20 mM Tris phosphate (pH 7.8), 1.07 mM $MgCl_2$, 2.67 mM $MgSO_4$, 0.1 mM EDTA, 33.3 mM DTT, 0.53 mM ATP, 0.47 mM luciferin, and 0.27 mM coenzyme A). The receptor activation potential of each compound was presented as fold induction measured as ratio of RLU of the compound over the RLU of the vehicle control.

Acknowledgments

The authors are grateful to the European Union (Anticancer Retinoids, QLK3-2002-02029), the MEC-Spain (SAF2004-07131, Contract to S.A.; SAF2007-63880-FEDER; Juan de la Cierva Contract to F.R.B.), Xunta de Galicia (Grant 08CSA052383PR from DXI+D+i; Consolidación 2006/15 from DXPCTSUG), the INCa, the ANR and the Ligue National Contre le Cancer (H.G., équipe labelisé) for financial support.

Supplementary data

Supplementary data associated with this article can be found, in the online version, at doi:10.1016/j.bmc.2009.05.035.

References and notes

1. Germain, P.; Staels, B.; Dacquet, C.; Spedding, M.; Laudet, V. *Pharmacol. Rev.* **2006**, *58*, 685.
2. Germain, P.; Chambon, P.; Eichele, G.; Evans, R. M.; Lazar, M. A.; Leid, M.; de Lera, A. R.; Lotan, R.; Mangelsdorf, D. J.; Gronemeyer, H. *Pharmacol. Rev.* **2006**, *58*, 712.
3. Germain, P.; Chambon, P.; Eichele, G.; Evans, R. M.; Lazar, M. A.; Leid, M.; de Lera, A. R.; Lotan, R.; Mangelsdorf, D. J.; Gronemeyer, H. *Pharmacol. Rev.* **2006**, *58*, 760.
4. Gronemeyer, H.; Laudet, V. *Protein Profile* **1995**, *2*, 1173.
5. Laudet, V.; Gronemeyer, H. *The Nuclear Receptor Facts Book*; Academic: San Diego, 2002.

6. de Lera, A. R.; Bourguet, W.; Altucci, L.; Gronemeyer, H. *Nat. Rev. Drug. Discovery* **2007**, *6*, 811.
7. Altucci, L.; Gronemeyer, H. *Nat. Rev. Cancer* **2001**, *1*, 181.
8. Henney, J. E. *JAMA* **2000**, *283*, 1131.
9. (a) Farol, L. T.; Hymes, K. B. *Exp. Rev. Anticancer Ther.* **2004**, *4*, 180; (b) Blumenschein, G. R., Jr.; Khuri, F. R.; von Pawel, J.; Gatzemeier, U.; Miller, W. H., Jr.; Jotte, R. M.; Le Treut, J.; Sun, S.-L.; Zhang, J. K.; Dziewanowska, Z. E.; Negro-Vilar, A. *J. Clin. Oncol.* **2008**, *26*, 1879; (c) Ramlau, R.; Zatloukal, P.; Jassem, J.; Schwarzenberger, P.; Orlov, S. V.; Gottfried, M.; Pereira, J. R.; Temperley, G.; Negro-Vilar, R.; Rahal, S.; Zhang, J. K.; Negro-Vilar, A.; Dziewanowska, Z. E. *J. Clin. Oncol.* **2008**, *26*, 1886.
10. Altucci, L.; Leibowitz, M. D.; Ogilvie, K. M.; de Lera, A. R.; Gronemeyer, H. *Nat. Rev. Drug Discovery* **2007**, *6*, 793.
11. Ostrowski, J.; Roalsvig, T.; Hammer, L.; Marinier, A.; Starrett, J. E.; Yu, K.-L.; Reczek, P. R. *J. Biol. Chem.* **1998**, *273*, 3490.
12. Gèhin, M.; Vivat, V.; Wurtz, J.-M.; Losson, R.; Chambon, P.; Moras, D.; Gronemeyer, H. *Chem. Biol.* **1999**, *6*, 519.
13. Germain, P.; Kammerer, S.; Pérez, E.; Peluso-Iltis, C.; Tortolani, D.; Zusi, F. C.; Starrett, J. E.; Lapointe, P.; Daris, J.-P.; Marinier, A.; de Lera, A. R.; Rochel, N.; Gronemeyer, H. *EMBO Rep.* **2004**, *5*, 877.
14. Chao, W.; Hobbs, P. D.; Jong, L.; Zhang, X.; Zheng, Y.; Wu, Q.; Shroot, B.; Dawson, M. I. *Cancer Lett.* **1997**, *115*, 1.
15. Yu, K.-L.; Ostrowski, J.; Chen, S.; Tramposch, K. M.; Reczek, P. R.; Mansuri, M. M.; Starret, J. E., Jr. *Bioorg. Med. Chem. Lett.* **1996**, *6*, 2865.
16. Bernard, A.; Bernardon, J.-M.; Delescluse, C.; Martin, B.; Lenoir, M.-C.; Maignan, J.; Charpentier, B.; Pilgrim, W. R.; Reichert, U.; Shroot, B. *Biochem. Biophys. Res. Commun.* **1992**, *186*, 977.
17. Zusi, F. C.; Vivat-Hannah, V.; Lorenzi, M. V. *Drug Discov.* **2002**, *7*, 1165.
18. Yu, K.-L.; Spinazze, P.; Ostrowski, J.; Currier, S. J.; Pack, E. J.; Hammer, L.; Roalsvig, T.; Honeyman, J. A.; Tortolani, D. R.; Reczek, P. R.; Mansuri, M. M.; Starret, J. E., Jr. *J. Med. Chem.* **1996**, *39*, 2411.
19. Klaholz, B. P.; Moras, D. *Structure* **2002**, *10*, 1197.
20. Klaholz, B. P.; Mitschler, A.; Moras, D. *J. Mol. Biol.* **2000**, *302*, 155.
21. Klaholz, B. P.; Mitschler, A.; Belema, M.; Zusi, C.; Moras, D. *Proc. Natl. Acad. Sci. U.S.A.* **2000**, *97*, 6322.
22. Chiba, H.; Clifford, J.; Metzger, D.; Chambon, P. *Mol. Cell. Biol.* **1997**, *17*, 3013.
23. (a) Peterson, V. J.; Barofsky, E.; Deinzer, M. L.; Dawson, M. I.; Feng, K.-C.; Zhang, X.-K.; Madduru, M. R.; Leid, M. *Biochem. J.* **2002**, *362*, 173; (b) Hughes, P. J.; Zhao, Y.; Chandraratna, R. A. S.; Brown, G. *J. Cell. Biochem.* **2006**, *97*, 327.
24. (a) Nagy, L.; Schwabe, J. W. R. *Trends Biomed. Sci.* **2004**, *29*, 317; (b) Hashimoto, Y.; Miyachi, H. *Bioorg. Med. Chem.* **2005**, *13*, 5080.
25. Bourguet, W.; Germain, P.; Gronemeyer, H. *Trends Pharmacol. Sci.* **2000**, *21*, 381.
26. Agarwal, C.; Chandraratna, R. A. S.; Johnson, A. T.; Rorke, E. A.; Eckert, R. L. *J. Biol. Chem.* **1996**, *271*, 12209.
27. Nahoum, V.; Pérez, E.; Germain, P.; Rodríguez-Barrios, F.; Manzo, F.; Kammerer, S.; Lemaire, G.; Hirsch, O.; Royer, C. A.; Gronemeyer, H.; de Lera, A. R.; Bourguet, W. *Proc. Natl. Acad. Sci. U.S.A.* **2007**, *104*, 17323.
28. Kagechika, H.; Kawachi, E.; Hashimoto, Y.; Shudo, K. *J. Med. Chem.* **1989**, *32*, 834.
29. Dawson, M. I.; Jong, L.; Hobbs, P. D.; Xiao, D.; Feng, K.-C.; Chao, W.-R.; Pan, C.; Fontana, J. A.; Zhang, X.-K. *Bioorg. Med. Chem. Lett.* **2000**, *10*, 1311.
30. Mathur, C.; Snow, M. S.; Young, K. M.; Pincock, J. A. *Tetrahedron* **1985**, *41*, 1509.
31. (a) Luche, J. L. *J. Am. Chem. Soc.* **1978**, *100*, 2226; (b) Luche, J. L.; Hahn, L. R.; Crabbé, P. *J. Chem. Soc., Chem. Commun.* **1978**, 601.
32. Chidambaran, R.; Kant, J.; Zhu, J.; Lajeunesse, J.; Sirard, P.; Ermann, P.; Schierling, P.; Lee, P.; Kronenthal, D. *Org. Proc. Res. Dev.* **2002**, *6*, 632.
33. Chen, J. Y.; Penco, S.; Ostrowski, J.; Balaguer, P.; Pons, M.; Starrett, J. E.; Reczek, P.; Chambon, P.; Gronemeyer, H. *EMBO J.* **1995**, *14*, 1187.
34. Vivat, V.; Zechel, C.; Wurtz, J.-M.; Bourguet, W.; Kagechika, H.; Umemiya, H.; Shudo, K.; Moras, D.; Gronemeyer, H.; Chambon, P. *EMBO J.* **1997**, *16*, 5697.
35. Germain, P.; Iyer, J.; Zechel, C.; Gronemeyer, H. *Nature* **2002**, *415*, 187.
36. Dawson, M. I. *Curr. Med. Chem.-Anti-Cancer Agents* **2004**, *4*, 199.
37. Chen, J.-Y.; Clifford, J.; Zusi, C.; Starret, J.; Tortolani, D.; Ostrowski, J.; Reczec, P. R.; Chambon, P.; Gronemeyer, H. *Nature* **1996**, *382*, 819.
38. Alvarez, S.; Germain, P.; Alvarez, R.; Rodríguez-Barrios, F.; Gronemeyer, H.; de Lera, A. R. *Int. J. Biochem. Cell Biol.* **2007**, *39*, 1406.
39. Bourguet, W.; Vivat, V.; Wurtz, J.-M.; Chambon, P.; Gronemeyer, H.; Moras, D. *Mol. Cell.* **2000**, *5*, 289.
40. Renaud, J.-P.; Rochel, N.; Ruff, M.; Vivat, V.; Chambon, P.; Gronemeyer, H.; Moras, D. *Nature* **1995**, *378*, 681.
41. Klaholz, B. P.; Renaud, J.-P.; Mitschler, A.; Zusi, C.; Chambon, P.; Gronemeyer, H.; Moras, D. *Nat. Struct. Biol.* **1998**, *5*, 199.
42. Million, K.; Tournier, F.; Houcine, O.; Ancian, P.; Reichert, U.; Marano, F. *Am. J. Respir. Cell Mol. Biol.* **2001**, *25*, 744.
43. Umemiya, H.; Kagechika, H.; Fukasawa, H.; Kawachi, E.; Ebisawa, M.; Hashimoto, Y.; Eisenmann, G.; Erb, C.; Pornon, A.; Chambon, P.; Gronemeyer, H.; Shudo, K. *Biochem. Biophys. Res. Commun.* **1997**, *233*, 121.
44. Umemiya, H.; Fukasawa, H.; Ebisawa, M.; Eyrolles, L.; Kawachi, E.; Eisenmann, G.; Gronemeyer, H.; Hashimoto, Y.; Shudo, K.; Kagechika, H. *J. Med. Chem.* **1997**, *40*, 4222.
45. Takahashi, B.; Ohta, K.; Kawachi, E.; Fukasawa, H.; Hashimoto, Y.; Kagechika, H. *J. Med. Chem.* **2002**, *45*, 3327.
46. Recent studies by gene expression profiling using DNA microarrays revealed the existence of two subclasses of retinoid synergists that act through RXR, one exhibiting the classical rexinoid profile (9-*cis*-retinoic acid like) and the other an alternative retinoid profile (all-*trans* -retinoic acid like). The former would increase apoptotic effects whereas the latter would increase retinoidal activity enhancing cell differentiation; see: Ishida, S.; Shigemoto-Mogami, Y.; Kagechika, H.; Shudo, K.; Ozawa, S.; Sawada, J.; Ohno, Y.; Inoue, K. *Mol. Cell Therap.* **2003**, *2*, 49–58.
47. Fillingham, J.; Greenblatt, J. F. *Cell* **2008**, *134*, 206.
48. Cozzini, P.; Kellogg, G. E.; Spyrakis, F.; Abraham, D. J.; Costantino, G.; Emerson, A.; Fanelli, F.; Gohlke, H.; Kuhn, L. A.; Morris, G. M.; Orozco, M.; Pertinhez, T. A.; Rizzi, M.; Sotriffer, C. A. *J. Med. Chem.* **2008**, *51*, 6237.
49. *Insight II*, 2000; Molecular Simulations; San Diego, 2000.
50. Pople, J. A. et al GAUSSIAN *98, Revision A.11.2*; Gaussian, Inc.: Pittsburgh, PA, 2001.
51. Bayly, C. I.; Cieplak, P.; Cornell, W. D.; Kollman, P. A. *J. Phys. Chem.* **1993**, *97*, 10269.
52. Cornell, W. D.; Cieplak, P.; Bayly, C. I.; Gould, I. R.; Merz, K. M.; Ferguson, D. M.; Spellmeyer, D. C.; Fox, T.; Caldwell, J. W.; Kollman, P. A. *J. Am. Chem. Soc.* **1995**, *117*, 5179.
53. Rodríguez-Barrios, F.; Pérez, C.; Lobatón, E.; Velázquez, S.; Chamorro, C.; San-Félix, A.; Pérez-Pérez, M. J.; Camarasa, M. J.; Pelemans, H.; Balzarini, J.; Gago, F. *J. Med. Chem.* **2001**, *44*, 1853.
54. Åqvist, J. *J. Phys. Chem.* **1990**, *94*, 8021.
55. Jorgensen, W. L.; Chandrasekhar, J.; Madura, J. D. *J. Chem. Phys.* **1983**, *79*, 926.
56. http://amber.scripps.edu/doc8, U. AMBER8.
57. Ryckaert, J. P.; Ciccoti, G.; Berendsen, H. J. C. *J. Comput. Phys.* **1977**, *23*, 327.